NATIONAL ADVISORY COMMITTEE FOR AERONAUTICS

TECHNICAL MEMORANDUM 1246

HYDRODYNAMIC PROPERTIES OF PLANING SURFACES AND FLYING BOATS

By N. A. Sokolov

Translation

"Materialy po Gidrodinamicheskomu Raschetu Glisserov i Gidrosamoletov." CAHI Report No. 149, 1932.

Washington
October 1950

ERRATA

N. 3229

NACA TM 1246

HYDRODYNAMIC PROPERTIES OF PLANING SURFACES
AND FLYING BOATS
By N. A. Sokolov

October 1950

Page 26, next to last line: The definition of b should be "wetted chord in motion."

Page 27, last line: The word "millimeters" should be "meters."

NATIONAL ADVISORY COMMITTEE FOR AERONAUTICS

TECHNICAL MEMORANDUM 1246

HYDRODYNAMIC PROPERTIES OF PLANING SURFACES AND FLYING BOATS*

By N. A. Sokolov

INTRODUCTION

The study of the hydrodynamic properties of planing bottoms of flying boats and seaplane floats is at the present time based exclusively on the curves of towing tests conducted in tanks.

In order to provide a rational basis for the test procedure in tanks and practical design data, a theoretical study must be made of the flow at the step and relations derived that show not only qualitatively but quantitatively the inter-relations of the various factors involved.

The general solution of the problem of the development of hydrodynamic forces during the motion of the seaplane float or flying boat is very difficult for it is necessary to give a three-dimensional solution, which does not always permit reducing the analysis to the form of workable computation formulas. On the other hand, the problem is complicated by the fact that the object of the analysis is concerned with two fluid mediums, namely, air and water, which have a surface of density discontinuity between them.

The theoretical and experimental investigations on the hydrodynamics of a ship cannot be completely carried over to the design of floats and flying-boat hulls, because of the difference in the shape of the contour lines of the bodies, and, because of the entirely different flow conditions from the hydrodynamic viewpoint. Thus in ship construction, only the hydrostatic forces are considered and the hydrodynamic lifting forces are entirely ignored; in flying-boat construction this procedure cannot be followed because

---

*"Materialy po Gidrodinamicheskomu Raschetu Glisserov i Gidrosamoletov." CAHI Report No. 149, 1932, pp. 1-39.

for the working speeds of the planing surface (of the order of 60 to 100 km/hr) the hydrodynamic forces take up the greatest part of the weight of the structure, only a small part of the weight being supported by the hydrostatic forces due to the water displacement.

This entire analysis was conducted on the assumption of two-dimensional flow. A picture of the flow about the seaplane float in the relative motion at the instant after rising on the step is given in figure 1. The lines of flow LD going from infinity and meeting at the surface of separation of the air and water mediums separate at point D, where they meet the float, the streamline of the air passing above, and flowing around the float along the line DCB; the particles of water, moving along the line DEB wet the contour of the float below. At point B, these two boundary lines of the gaseous and liquid mediums again meet forming the separating surface BH.

In the case of the flow about a two-step planing bottom in a two-dimensional ideal flow, the flow picture will have a somewhat different appearance (fig. 2). The air particles lying on the line of flow (separating surface) LD will, as before, flow about the above-water part of the body DCF. The water particles meeting on the streamline LD in contact with the particles of air wet the surface of the body starting at the point D. At point B, the water particles leave the contour of the planing surface, wet the rear part BKN (in an actual flow, the region of suction), and at point N they again meet the surface, leave it at point F and continue along the separating surface FH.

In an actual flow for a finite span of the planing surface, the flow picture in the above-water part will differ considerably from the picture just given but the flow picture of the below-water part remains essentially the same.

This paper develops, in general form, the lift and drag equations for the motion of a solid body on a separating surface. Then, considering the solid body as a half-submerged flat plate, these formulas are modified somewhat and the lift and drag formulas for the planing flat plate are obtained. By evaluating the experimental data, the analytical expressions are supplemented with test curves and finally all data required for the hydrodynamic computation of a seaplane float or flying boat with a flat bottom are obtained.

1. MOTION OF SOLID BODY AT BOUNDARY OF TWO FLUID MEDIUMS OF DIFFERENT DENSITY

In the general case, this problem may be formulated as follows:

The solid body A moves forward with constant velocity V_0 in such a manner that at all times during the motion the part DCB is in the fluid medium I of density ρ_1; whereas the part bounded by the contour DEB is in the fluid medium II of density ρ_2 (fig. 3).

In considering the relative motion, it is assumed that the x-axis coincides with the surface separating the fluids in the undisturbed state and is directed along in the direction of motion, the y-axis being at right angles and directed up.

The flows are assumed two-dimensional; both flows are potential, and the separating surface in the relative motion is fixed.

In passing from fluid I to fluid II, there is a discontinuity in the density and in the first derivatives of the pressure with respect to the coordinates. Moreover, there is a velocity discontinuity at the separating surface. At an infinite distance in front of the body, both fluids are assumed to be relatively at rest; physically this assumption is comparable to assuming that in the motion of the solid body over the water surface there is no tail or head wind.

Because medium I possesses all the properties of two-dimensional flow, the usual hydrodynamic equations of two-dimensional flow can be applied and the resultant pressure from flow I, on the portion of body A which is bounded by the line BCD and wetted by fluid I, can be obtained. The resultant pressure of flow II on the remaining part of body A, which is bounded by the contour DEB and wetted by fluid II, can be found by means of a similar manner of operation with medium II. The total force exerted on the body by fluids I and II is equal to the geometric sum of the forces exerted separately on the moving body by each flow.

In the following discussion, all the results are expressed in terms of fluid II. The final formulas for medium I will be the same as for medium II except for change in the contour of integration and replacement of ρ_2 and γ_2 by ρ_1 and γ_1, indicating that the mass and weight densities are now referred to medium I. For convenience the subscripts indicating that the magnitudes refer to medium II are omitted.

For steady motion with velocity potential, the pressure at any point of the wetted contour BED by medium II is determined by the Bernoulli-Lagrange equation

$$p = C - \rho \frac{V^2}{2} - \gamma y \tag{1}$$

The components of the pressure along the coordinate axes for the element ds of the contour may be written

$$np_\alpha(pds) = \left(- C + \rho \frac{V^2}{2} + \gamma y\right) dy$$

$$np_y(pds) = \left(C - \rho \frac{V^2}{2} - \gamma y\right) dx$$

The components of the force P_2 exerted on the solid body by medium II along the axis are obtained by integrating these expressions over the contour BED. These components are denoted by X_2 and Y_2; then

$$\left.\begin{aligned} X_2 &= - \int_{BED} C\, dy + \int_{BED} \gamma y\, dy + \frac{\rho}{2} \int_{EDB} V^2\, dy \\ Y_2 &= \int_{BED} C\, dx - \int_{BED} \gamma y\, dx - \frac{\rho}{2} \int_{BED} V^2\, dx \end{aligned}\right\} \tag{2}$$

The Bernoulli constant C is determined by the conditions at infinity ($y = 0$, $V = V_0$, $p = p_0$) and is given by

$$C = p_0 + \rho \frac{V_0^2}{2} \tag{3}$$

In medium II, let the flow be determined by the complex potential function

$$W_2 = \varphi_2 + i\psi_2$$

where φ_2 is the velocity potential and ψ_2 is the stream function.

With regard to the velocity potential φ, it should be noted that for flows I and II the form proposed by N. E. Joukowsky, for the flow about a wing, will be used:

$$\varphi = - V_0 x + f(x,y)$$

where $f(x,y)$ is a function of the coordinates that satisfy the Laplace equation.

With regard to the function $f(x,y)$, the following point may be made: The derivatives of the function $f(x,y)$, $\partial f/\partial x$, and $\partial f/\partial y$, which give the added (disturbance) flow velocities produced by the moving body, have these properties: At an infinite distance in front of the moving body and below and above the body, the derivatives are of the order of smallness $1/R$; at an infinite distance behind the moving body, but sufficiently near the separation surface, the derivatives are finite.

In the motion of a body of a homogeneous-infinite fluid the derivatives $\partial f/\partial x$ and $\partial f/\partial y$, everywhere with increasing distance from the body, are of the order of smallness $1/R$.

Because the line BED is a streamline,

$$d\varphi = V ds$$

$$d\psi = 0$$

Add to the right side of the expression for X_2 the sum of the terms

$$\frac{\rho}{2}\int_{BED}\left[2V_0\frac{\partial f}{\partial x}\,dy - 2\left(\frac{\partial f}{\partial x}\right)^2 dy + 2\frac{\partial f}{\partial x}\frac{\partial f}{\partial y}\,dx\right] = -\rho\int_{BED}\frac{\partial f}{\partial x}\,d\psi$$

and correspondingly for Y_2

$$\frac{\rho}{2}\int_{BED}\left[2V_0\frac{\partial f}{\partial y}\,dy + 2\left(\frac{\partial f}{\partial y}\right)^2 dx - \frac{\partial f}{\partial x}\frac{\partial f}{\partial y}\,dy\right] = -\rho\int_{BED}\frac{\partial f}{\partial y}\,d\psi$$

Both of the added expressions are equal to zero inasmuch as for the streamline BED $d\psi = \left(-V_0 + \frac{\partial f}{\partial x}\right)dy - \frac{\partial f}{\partial y}\,dx = 0$ so that equations (2) still hold.

Because

$$V^2 = V_0^2 - 2V_0\frac{\partial f}{\partial x} + \left(\frac{\partial f}{\partial x}\right)^2 + \left(\frac{\partial f}{\partial y}\right)^2$$

equations (2) can be rewritten separating the terms in the following manner:

$$\left.\begin{aligned} X_2 &= -p_0\int_{BED} dy + \gamma\int_{BED} y\,dy - \frac{\rho}{2}\int_{BED}\left[\left(\frac{\partial f}{\partial x}\right)^2 dy - \left(\frac{\partial f}{\partial y}\right)^2 dy - 2\frac{\partial f}{\partial x}\frac{\partial f}{\partial y}\,dx\right] \\ Y_2 &= p_0\int_{BED} dx - \gamma\int_{BED} y\,dx + \frac{\rho}{2}\int_{BED}\left[\left(\frac{\partial f}{\partial y}\right)^2 dx - \left(\frac{\partial f}{\partial x}\right)^2 dx - 2\frac{\partial f}{\partial x}\frac{\partial f}{\partial y}\,dy\right] + \\ &\qquad \rho V_0\int_{BED}\left[\frac{\partial f}{\partial x}\,dx + \frac{\partial f}{\partial y}\,dy\right] \end{aligned}\right\} \quad (5)$$

The corresponding expressions for X_1 and Y_1 can be obtained for fluid I, X_1, and Y_1 being obtained from X_2 and Y_2 by replacing ρ_2, γ_2 by ρ_1, γ_1 and the contour of integration BED by the contour DCB.

The similar terms of the expressions for X_2 and Y_2 shall be considered in pairs and by analogy the same terms for medium I.

The first sums of the integrals for the mediums I and II

$$p_0 \int_{DCB} dx + p_0 \int_{BED} dx = 0$$

and

$$p_0 \int_{DCB} dy + p_0 \int_{BED} dy = 0$$

are equal to zero because the integrals of dx and dy are taken over the closed contour DCBED.

The following terms of equations (5) will be considered; they are correspondingly denoted by X_{1F}, X_{2F}, Y_{1F}, and Y_{2F} where

$$\left.\begin{aligned} X_{1F} &= \gamma_1 \int_{DCB} y\,dy \\ X_{2F} &= \gamma_2 \int_{BED} y\,dy \\ Y_{1F} &= -\gamma_1 \int_{DCB} y\,dx \\ Y_{2F} &= -\gamma_2 \int_{BED} y\,dx \end{aligned}\right\} \qquad (6)$$

These expressions, in general, give the resistance forces and the lift forces due to the hydrostatic pressure on the wetted contours DCB and BED.

In computing the lift forces Y_{1F} and Y_{2F}, it is necessary to consider the following:

The volumes $\int ydx$ for medium I are taken between the contour DCB and the x-axis, which is the water-line of the motion. The volumes lying below the water-line are taken with the minus sign (fig. 4). For medium II, the rule of computation is the opposite, the volumes lying above the x-axis (for example, the area DdD') are negative.

Introducing the notation

$$\left.\begin{aligned} F_1 &= \text{area } B'CDD'B' \\ F_2 &= \text{area } B'D'EBB' \\ F_3 &= \text{area } D'DdD' \\ F_4 &= \text{area } BbB'B \end{aligned}\right\} \tag{7}$$

for the forces Y_{1F} and Y_{2F}, the following expressions are obtained:

$$\left.\begin{aligned} Y_{1F} &= \gamma_1 (F_1 + F_3 - F_4) \\ Y_{2F} &= \gamma_2 (F_2 + F_4 - F_3) \end{aligned}\right\} \tag{8}$$

Finally, X_{1F} and X_{2F} give the projection on the x-axis of the hydrostatic pressures of fluids I and II on the contours DCB and BED. By denoting the projections of BED' and BED on the y-axis by b_{0y} and b_y, or by h_1 and h_2, the ordinates of the points D and B can be obtained for X_{1F} and X_{2F}.

$$\left.\begin{aligned} X_{1F} &= \gamma_1 \frac{h_1^2 - h_2^2}{2} = \gamma_1 \frac{b_y(2b_{0y} - b_y)}{2} \\ X_{2F} &= \gamma_2 \frac{h_2^2 - h_1^2}{2} = -\gamma_2 \frac{b_y(2b_{0y} - b_y)}{2} \end{aligned}\right\} \tag{9}$$

The force X_{1F} is directed along the motion; the force X_{2F}, which is a resistance, is directed opposite the motion.

In the case of the motion of a body in a homogeneous fluid ($\gamma_1 = \gamma_2$), equations (8) and (9) give the lift force equal to the water displacement of the body and, as was to be expected, a resistance equal to zero:

$$\left.\begin{aligned} Y_F &= Y_{1F} + Y_{2F} = \gamma \cdot (F_1 + F_2) = \gamma F \\ X_F &= X_{1F} + X_{2F} = \gamma \frac{h_2^2 - h_1^2}{2} + \gamma \frac{h_1^2 - h_2^2}{2} = 0 \end{aligned}\right\} \tag{10}$$

In determining the forces acting on a wing moving through air, the fluid is assumed to be weightless and for the wing the hydrostatic lift force is negligibly small.

By returning to equations (5)

$$\left.\begin{aligned} X_{2N} &= -\frac{\rho}{2} \int_{BED} \left[\left(\frac{\partial f}{\partial x}\right)^2 dy - \left(\frac{\partial f}{\partial y}\right)^2 dy - 2 \frac{\partial f}{\partial x} \frac{\partial f}{\partial y} dx \right] \\ Y_{2N} &= \frac{\rho}{2} \int_{BED} \left[\left(\frac{\partial f}{\partial y}\right)^2 dx - \left(\frac{\partial f}{\partial x}\right)^2 dx - 2 \frac{\partial f}{\partial x} \frac{\partial f}{\partial y} dy \right] \\ Y_{2J} &= \rho V_0 \int_{BED} \left[\frac{\partial f}{\partial x} dx + \frac{\partial f}{\partial y} dy \right] = \rho v_0 \int_{BED} df \end{aligned}\right\} \tag{11}$$

The physical interpretation that must be given to the obtained formulas in the limiting case where the densities of the fluids are equal; that is, when the body moves through a homogeneous fluid, will be considered. As the contours of integration, for fluid I the contour DLWHB shall be considered and for fluid II the contour BHVLD. The sum of these contours is equal to the circle LWHV of infinitely large radius and they have two branches, DL and BH lying in the surface of separation of the fluids, extending to infinity. In the limiting case of a homogeneous fluid ($\rho_1 = \rho_2$), the surfaces DL and BH are not surfaces of separation and there is no discontinuity in velocity or density (fig. 5).

The possibility of replacing the contours DCB and BED, respectively, by DLWHB and BHVLD, will now be considered.

The pair of contours DCB + BHVLD and BED + DLWHB give the two closed contours DCBHVLD and BEDLWHB.

It shall now be proven that the expressions X_N and Y_N taken for the closed contours are equal to zero. For this proof, it is sufficient to show that the expressions under the integral sign are the total differentials of certain functions, that is,

$$\frac{\partial}{\partial x}\left[\left(\frac{\partial f}{\partial x}\right)^2 - \left(\frac{\partial f}{\partial y}\right)^2\right] = -2\frac{\partial}{\partial y}\left(\frac{\partial f}{\partial x}\frac{\partial f}{\partial y}\right)$$

$$\frac{\partial}{\partial y}\left[\left(\frac{\partial f}{\partial y}\right)^2 - \left(\frac{\partial f}{\partial x}\right)^2\right] = -2\frac{\partial}{\partial x}\left(\frac{\partial f}{\partial x}\frac{\partial f}{\partial y}\right)$$

By expanding these expressions, the following relations are obtained:

$$\frac{\partial f}{\partial x}\left(\frac{\partial^2 f}{\partial x^2} + \frac{\partial^2 f}{\partial y^2}\right) = 0$$

$$\frac{\partial f}{\partial y}\left(\frac{\partial^2 f}{\partial x^2} + \frac{\partial^2 f}{\partial y^2}\right) = 0$$

The function $f(xy)$ by hypothesis satisfies the Laplace equation; thus, it has been shown what was required so that the contours DCB and BED are replaceable by the contours BHVLD and DLWHB, respectively. It is merely necessary to change the sign before the integral for the described direction of going around the contour.

The same substitution is permissible for the expression Y_J because the function under the integral gives the circulation over an element of the contour due to the added flow $f(xy)$. The circulation due to the added flow for any closed contour lying entirely in the fluids I and II is equal to zero for there are no vortices within the fluid.

By integrating the terms X_N and Y_N over the lines DL and BH once for fluid I and a second time for fluid II, the sum zero is obtained because the order of describing these contours of integration for the fluids I and II are opposite.

On integrating the same terms X_N and Y_N over the circle LWHV of infinitely large radius, an infinitely small magnitude of the order $1/R$ results because $\partial f/\partial x$ and $\partial f/\partial y$, in the case of motion of the body in a homogeneous fluid without a surface of discontinuity, are of the order of smallness $1/R$. Thus, the terms X_N and Y_N are equal to zero for the motion of a body in a homogeneous fluid.

Further, the term $Y_J = \rho V_0 \int df$ taken for the fluid I over the contour BHVLD and for fluid II over the contour DLWHB gives as a result the expression

$$Y_J = \rho V_0 J \tag{12}$$

where J is the circulation of the fluid over any contour that includes the contour of the moving body. It is not difficult to see that the terms Y_J taken over the lines DL and BH cancel, for, in this case, the directions of passing around the contours of integration for the fluids I and II are opposite.

In the general case of the motion of a body in a homogeneous, weightless, and incompressible fluid, the result leads, as was to be expected, to the theorem of N. E. Joukowsky on the lift of an airfoil.

The physical meaning that must be given to the obtained formulas for the motion of a solid body on the boundary of two fluid mediums in the presence of the surface of discontinuity DL and HB will now be investigated.

Consider the terms

$$X_N = X_{1N} + X_{2N}$$

$$Y_N = Y_{1N} + Y_{2N}$$

where X_N and Y_N are given by equations (11).

It has been shown that in the case of the motion of a body in a homogeneous fluid, the velocities of the additional flow $\partial f/\partial x$ and $\partial f/\partial y$, having the order of smallness $1/R$, give on integrating over a contour of infinite radius zero for the terms X_N and Y_N.

In the motion of a body on the surface of separation of two heavy fluids, the picture is somewhat different. The wave surface behind the moving body does not decrease the amplitudes of its waves because the case of the motion of an ideal fluid is being considered. For this reason, the velocities of the additional flow, even at an infinite distance from the body but sufficiently near the surface of separation, have a finite value and the terms X_N and Y_N do not give zero on integration.

It was impossible to reduce the expressions X_N and Y_N to a shorter and simpler form. In what follows the term X_N shall be denoted as the form drag. The form drag gives the projection on the x-axis of the resultant hydrodynamic pressure of an ideal fluid on the wetted contour without taking account of the hydrostatic pressure.

The term Y_N shall be considered in detail later in this report.

The last terms considered have the expression

$$Y_J = Y_{1J} + Y_{2J} \tag{13}$$

where

$$\left.\begin{aligned} Y_{1J} &= \rho_1 V_0 \int_{DCB} df = \rho_1 V_0 J_1 \\ Y_{2J} &= \rho_2 V_0 \int_{BED} fd = \rho_2 V_0 J_2 \end{aligned}\right\} \tag{14}$$

Physically, these expressions give the magnitude of the lift force due to the circulation of the fluid and are equal to the circulation about the wetted contour multiplied by the density of the fluid and velocity of the flow at infinity. The theorem of N. E. Joukowsky, in a somewhat different form, has thus been obtained; namely, in the motion of a body on the surface of separation of two fluid mediums of different density, the lift force due to the circulation is equal to the sum of the two forces each of which is determined as the product of the circulations over the wetted contour multiplied by the density of the given fluid and the flow velocity at infinity.

In summarizing, the forces acting on a solid body moving half submerged on the surface of separation of two heavy fluid mediums I and II with densities ρ_1 and ρ_2 may be expressed as follows:

The total resistance force is equal to

$$X = X_{1F} + X_{2F} + X_{1N} + X_{2N} \tag{15}$$

where

$$\left.\begin{aligned} X_{1F} &= \gamma_1 \frac{h_1^2 - h_2^2}{2} \\ X_{2F} &= -\gamma_2 \frac{h_1^2 - h_2^2}{2} \\ X_{1N} &= -\frac{\rho_1}{2} \int_{DCB} \left[\left(\frac{\partial f}{\partial x}\right)^2 dy - \left(\frac{\partial f}{\partial y}\right)^2 dy - 2 \frac{\partial f}{\partial x} \frac{\partial f}{\partial y} dx \right] \\ X_{2N} &= -\frac{\rho_2}{2} \int_{BED} \left[\left(\frac{\partial f}{\partial x}\right)^2 dy - \left(\frac{\partial f}{\partial y}\right)^2 dy - 2 \frac{\partial f}{\partial x} \frac{\partial f}{\partial y} dx \right] \end{aligned}\right\} \tag{16}$$

The forces X_{1F} and X_{2F} give the projections on the x-axis of the hydrodynamic force on the wetted contour.

The forces X_{1N} and X_{2N} are the form drags.

The total lift force is expressed by

$$Y = Y_{1F} + Y_{2F} + Y_{1N} + Y_{2N} + Y_{1J} + Y_{2J} \tag{17}$$

where

$$\left.\begin{aligned}
Y_{1F} &= \gamma_1 (F_1 + F_3 - F_4) \\
Y_{2F} &= \gamma_2 (F_2 - F_3 + F_4) \\
Y_{1N} &= \frac{\rho_1}{2} \int_{DCB} \left[\left(\frac{\partial f}{\partial y}\right)^2 dx - \left(\frac{\partial f}{\partial x}\right)^2 dx - 2 \frac{\partial f}{\partial x} \frac{\partial f}{\partial y} dy \right] \\
Y_{2N} &= \frac{\rho_2}{2} \int_{BED} \left[\left(\frac{\partial f}{\partial y}\right)^2 dx - \left(\frac{\partial f}{\partial x}\right)^2 dx - 2 \frac{\partial f}{\partial x} \frac{\partial f}{\partial y} dy \right] \\
Y_{1J} &= \rho_1 V_0 \int_{DCB} df = \rho_1 V_0 J_1 \\
Y_{2J} &= \rho_2 V_0 \int_{BED} df = \rho_2 V_0 J_2
\end{aligned}\right\} \tag{18}$$

Forces Y_{1F} and Y_{2F} give the volumes of the displaced liquids I and II.

Forces Y_{1N} and Y_{2N} give the lift forces due to the shape of the vessel.

Forces Y_{1J} and Y_{2J} give the lift forces due to the circulation.

The test results shall now be considered and the formulas obtained shall be applied to the case of a flat half-submerged plate; the results obtained at the Hamburg towing basin by Sottorf shall be used.

The order of the component forces is determined in percentage of the total lift force and resistance. The curves of figures 6 and 7 give this relation and refer to a flat plate towed with constant velocity (V_0 = 6 m/sec) for a constant vertical load (Y = 18 kg) and having a span at right angles to the direction of motion (l = 0.3 m). The forces were computed only for water; the aerodynamical forces were not taken into account.

Inspection of these curves permits the following conclusions to be drawn:

1. Equation (17) gives for the lift forces three components: the hydrostatic, the one due to circulation, and the one due to form. The numerical computation given and figure 6 show that the lift force Y_N, due to the form, is practically zero. (In the computation the magnitude, Y_N constituted no more than 3 percent with some fluctuations on either side due to the inaccuracy of the computation procedure.) In this case, the total lift force of a solid body is equal to the sum of two forces: (1) the hydrostatic force Y_F and (2) the force due to the circulation Y_J, which gives the physical analogy to the theorem of Joukowsky where the total lift force for the solid body moving in a homogeneous fluid is equal to the sum of the circulation and the hydrostatic forces. The hydrostatic force, due to its relative smallness for air, is generally neglected.

An assumption based on a comparison of the results of tests is expressed here. A strict proof that the lift force Y_N is equal to zero was not obtained. A deeper analysis of the essential nature of the flow about a solid body at the surface of separation will permit determining more fully the magnitude and the character of the force Y_N. It should be noted that equating the term Y_N to zero permitted deriving the analytical relation for certain magnitudes characterizing the resistance of a moving plate, in

particular, the resistance X_N. Comparison with the test results given by Sottorf confirmed the correctness of the conclusion as to the zero value of Y_N, and the character of the test curves for increasing span of the plate agrees with the obtained analytical expression for infinite span.

2. The hydrostatic lift force, which for small angles of attack assumes a considerable part of the load, rapidly drops with increasing angle of attack, practically reaching zero at the angle of attack $\alpha = 10^\circ$.

3. The hydrodynamic lift force, due to the circulation, is small at small angles of attack, rapidly increases with α, and at 10° practically assumes the entire vertical load.

Both of these conclusions become physically understandable if a disturbance in the flow arising from the change in the angle of attack of the plate is considered. At the angle of attack α near zero the disturbance in the flow is small; the streamlines practically maintain their horizontal direction and the circulation due to the added flow of velocity potential $f(xy)$ over the wetted contour is very small. At this instant, the entire load of the plate can be and is taken up only by the hydrostatic lift forces. With increasing angle of attack, the plate becomes more submerged in the fluid, the circulation of the added flow increases, and therefore the circulation lift force increases. At the same time, the value of the hydrostatic force relatively decreases because the hydrostatic force normal to the plate gives, with increasing angle of attack, a relatively smaller vertical component.

The resistance of the flat plate in moving half submerged in a fluid consists of the surface friction drag, the hydrostatic resistance, and the form drag. Figure 7 shows relative change of these forces. The induced drag due to the shed vortices, in the case of a finite span of the plate, will not be considered because the coefficients derived on the basis of test results already include the effect of vortex formation on the planing flat plate.

The following conclusions, which are in full agreement with these preceding results, may be derived:

4. The friction drag was computed by use of formulas that take into account the velocity distribution on the surface of the plate and the Reynolds number (see formulas that follow). At small angles of attack, the friction drag constitutes a large part of the total

resistance and is of the order of 6 percent for the angle of attack $\alpha = 10^{\circ}$. This drop is essentially explained by the decrease in the wetted surface with increasing angle of attack. In correspondence with the results of tests, the turbulent state of the surface friction was assumed here.

5. The hydrostatic resistance has, in general, a small value. At $\alpha = 0^{\circ}$, the value is practically zero; it increases reaching a maximum at $\alpha = 2.5^{\circ}$ and then drops almost to zero at $\alpha = 10^{\circ}$. This effect is understandable if the fact that the rise of the fluid (to point D, fig. 4) decreases the magnitude of the hydrostatic pressure is considered.

6. The hydrodynamic resistance X_N, termed the "form drag," is zero at $\alpha = 0^{\circ}$ and increases with α reaching 93 percent of the total resistance of the plate at $\alpha = 10^{\circ}$. The explanation of this phenomenon lies in the fact, that with increasing angle of attack there is an increase of that, which in aerodynamics is termed the "frontal area" of the plate, that is, the projection of the wetted surface, on a plate perpendicular to the direction of motion. At large angles of attack, there is a greater deceleration of the flow, hence, an increase in resistance X_N.

The present work may be viewed as an attempt to investigate hydrodynamically the nature of the phenomenon of the motion of a solid body on the surface of separation of two fluid mediums of different densities. The consideration of the general case of the motion of a solid body is now concluded. In the next section, the general formulas obtained are applied to the motion of a flat plate and on the basis of experimental data test curves are presented that permit the computation of the planing plate.

2. MOTION OF HALF-SUBMERGED FLAT PLATE ON SURFACE OF HEAVY FLUID

In the motion of a seaplane or flying boat on the surface of water, after rise on the step, the hydrodynamic lift forces assume the larger part of the total weight and only a very small part of the total weight of the structure is supported by the hydrostatic force (force of water displacement).

At the velocity of motion of a planing surface equal to zero, the entire structure is balanced by the hydrostatic lift forces.

Thereafter with increasing velocity (fig. 8), due to the hydrodynamic forces that arise, the planing surface begins gradually to rise out of the water in such a manner that the sum of the hydrodynamic lift forces and the water displacement forces is at all times equal to the weight of the float. At the velocity $V = V_1$, it is assumed that the bottom has come out on the step, that is, the initial weight is taken up by the hydrodynamic lift forces, and that the water displacement is not large and can be neglected. Actually, the water displacement of the body drops with the velocity and would become zero at $V = \infty$.

The contours of the bottom lines of planing bottoms in the immediate neighborhood of the step closely approximate those of a flat plate. This fact permits the supporting part of the bottom of a seaplane, after coming out on the step, to be considered as a flat plate moving half submerged at the angle of attack α with the horizontal because the character of the motion is sufficiently like that of a two-dimensional flow.

In the case of the motion of a two-step body, the rear step meets the surface of the water already disturbed by the forward step and therefore the angle of attack of the rear step will not be equal to the angle between the line of the bottom and the water line of the motion. The choice of the optimum angle of attack at the rear step should be made on the basis of a special analysis of the phenomenon of the flow about the bottom at the rear step. In the given case, this report is restricted to the consideration of the flow about the bottom at the forward step.

Let the flat plate of infinite width, submerged to the length b_0, move with velocity V_0 over the water surface at the angle of attack α to the horizontal. As is shown by experiment, the wetting of the surface of the moving plate starts not at point E (fig. 9), which is determined by the intersection of the horizontal with the plate, but somewhat higher, namely, at point D. The ratio $b = BD$ to $b_0 = BE$ is a certain function of the angle of attack, the velocity of motion and the depth of submergence of the plate.

The present discussion considers the coordinate points as known and, therefore, the true wetted area $S = lb$ is known. At the end of this paper it will be shown how the value of the ratio b/b_0 may be approximately determined.

Application of equations (15) and (17), derived in the general case for the solid body of arbitrary shape moving on the surface of

separation of two fluids, will now be made to the motion of the partly submerged flat plate. In applying the obtained results to the particular problem of constructing the graph of the lift and drag forces of a flying boat hull or seaplane float during take-off on water, this paper is restricted to the determination of the forces acting on the plate due only to the water and not the aerodynamic forces, which in view of the variety of shapes of the above water parts may be more reliably obtained from special wind-tunnel tests on models. Thus, in all the following equations ρ_1 and γ_1 will not appear and ρ_2 and γ_2, now denoted by ρ and γ, will correspond to the mass and weight density of the water.

The kinematic condition for the line of flow LDEBH coinciding with the part DEB of the plate (fig. 9) may be written

$$\frac{\partial\varphi}{\partial y} : \frac{\partial\varphi}{\partial x} = \operatorname{tg}\alpha = \frac{dy}{dx} \tag{19}$$

where α denotes the angle of attack of the plate. In what follows a new magnitude ϵ, which shall be denoted as the mean relative retardation of the flow over the part DEB, will be introduced. Thus, by denoting the total velocity of the flow at the streamline by V and the flow velocity at infinity by V_0, the retardation will equal the difference:

$$\Delta V = V_0 - V$$

and the mean relative retardation ϵ, the arithmetic mean of the magnitude $\Delta V/V_0$ over the contour DEB is

$$\epsilon = \left(\frac{\Delta V}{V_0}\right)_{cp} = \int_{BED} \frac{\Delta V}{V_0}\,\frac{db}{b} \tag{20}$$

By applying equations (15) and (17) to the case of the motion of a partly submerged plate, the hydrostatic lift and drag forces, expressed by the following formulas, are obtained:

$$\left.\begin{aligned} X_F &= -0.5\,\gamma \sin^2 \alpha b\,(2b_0 - b) \\ Y_F &= 0.25\,\gamma \sin 2\alpha b\,(2b_0 - b) \end{aligned}\right\} \tag{21}$$

where the forces are referred to unit length of the plate in the direction of the span.

In order to express the terms X_N, Y_N, and Y_J as a function of the ratio ϵ, the expressions of the magnitudes under the integral signs in equations (15) and (17) shall be written as functions of ϵ. Because the contour BED is a streamline (fig. 10), the following relations may be written.

$$\frac{\partial f}{\partial x} = V_0 - V\cos\alpha = -V_0\left[1 - (1 - \epsilon)\cos\alpha\right]$$

$$\frac{\partial f}{\partial y} = -V\sin\alpha = -V_0(1 - \epsilon)\sin\alpha$$

By substituting the expressions obtained for $\partial f/\partial x$ and $\partial f/\partial y$ in equations (15) and (17) and after some transformations, the following equations are obtained:

$$\left.\begin{aligned} X_N &= -\epsilon(2 - \epsilon)\sin\alpha\,\frac{\rho}{2}\,bV_0^2 \\ Y_N &= \left[\epsilon(2 - \epsilon)\cos\alpha - 2(\cos\alpha + \epsilon - 1)\right]\frac{\rho}{2}\,bV_0^2 \\ Y_J &= 2(\cos\alpha + \epsilon - 1)\,\frac{\rho}{2}\,bV_0^2 \end{aligned}\right\} \tag{22}$$

In these equations, and also in all equations given hereafter, a certain assumption is made; namely, the integral of the squares of the ratio $\Delta V/V_0$ were substituted by the square of the mean ratio $\Delta V/V_0$, that is,

$$\int_{BED} \left(\frac{\Delta V}{V_0}\right)^2 \frac{db}{b} = \left(\frac{\Delta V}{V_0}\right)^2_{cp} = \epsilon^2$$

Actually, if $\Delta V/V_0 = \epsilon + \Delta\epsilon$, substitution in the integral gives

$$\int_{BED} \left(\frac{\Delta V}{V_0}\right)^2 \frac{db}{b} = \int_{BED} (\epsilon + \Delta\epsilon)^2 \frac{db}{b} =$$

$$\epsilon^2 \int_{BED} \frac{db}{b} + 2\epsilon \int_{BED} \Delta\epsilon \frac{db}{b} + \int_{BED} (\Delta\epsilon)^2 \frac{db}{b}$$

The first integral on the right gives ϵ^2; the second integral gives zero, because by definition $\int \Delta\epsilon \, db/b = 0$, and finally $\int (\Delta\epsilon)^2 \, db/b$ gives a positive quantity, which, however, is so small that it may be neglected. Thus, for coefficients of the order of unity, this quantity in the most unfavorable case will amount to several thousandths and therefore with a sufficient degree of accuracy the following equation may be written:

$$\int_{BED} \left(\frac{\Delta V}{V_0}\right)^2 \frac{db}{b} = \left(\frac{\Delta V}{V_0}\right)^2_{cp} = \epsilon^2 \qquad (23)$$

Thus, for a given angle of attack and a given wetted area, the lift force from the circulation Y_J and the forces Y_N and X_N

can be computed, if the mean relative retardation ϵ for given parameters of the motion is known.

The dependence of the ratio ϵ on the angle of attack α and the wetted area will be established later when the experimental data obtained by Sottorf at the Hamburg towing basin are considered. For the present, the derivation of further formulas, which are required for the practical computation of the problem of a planing bottom, shall be regarded.

Up to now, the phenomenon in an ideal fluid, without taking account of the friction, has been considered. In the case of the motion of a solid body (plate) on the boundary of real (viscous) fluids, it is necessary to add to the forces already determined the force due to the friction at the surface of the body. The formulas for the friction force of a planing flat plate will be derived. Investigations on the surface friction have shown that the friction on an element of surface of area dS is expressed in the following form

$$dR = C_f \frac{\rho}{2} V^2 dS \tag{24}$$

where C_f is a coefficient, which depends on the Reynolds number, and V is the flow velocity at a given point of the wetted area.

The dependence of the coefficient of friction on the Reynolds number, according to the latest investigations of the friction of flat plates, will vary with the flow regime (fig. 11, reference 1).

For smooth polished plates for flow regimes with Reynolds number $Re < 5 \cdot 10^5$, the dependence of C_f on Re has the following form (curve b):

$$C_f = \frac{1.327}{\sqrt{Re}} \tag{25}$$

For the motion of the same plate with Reynolds number $Re > 5 \cdot 10^5$, the laminar flow, with increasing Reynolds

number, gradually goes over into turbulent flow and the dependence of C_f on Re is expressed by the formula of Prandtl (curve c):

$$C_f = \frac{0.074}{\sqrt[5]{Re}} - \frac{1700}{Re} \tag{26}$$

For a plate with blunt leading edges or with roughness that produces turbulence, the test data give the dependence of C_f on Re in the following form (curve a):

$$C_f = \frac{0.072}{\sqrt[5]{Re}} \tag{27}$$

Integrating equation (24) over S and replacing V by $V_0 - \Delta V$, the following is obtained for the plate of wetted area $S = lb$:

$$R = C_f (1 - \epsilon)^2 \frac{\rho}{2} S V_0^2 \tag{28}$$

The friction R is tangent to the plate so that its components along the axes of coordinates will be

$$\left.\begin{aligned} X_R &= - C_f (1 - \epsilon)^2 \cos \alpha \frac{\rho}{2} S V_0^2 \\ Y_R &= - C_f (1 - \epsilon)^2 \sin \alpha \frac{\rho}{2} S V_0^2 \end{aligned}\right\} \tag{29}$$

The coefficient $(1 - \epsilon)^2 \cos \alpha$ gives the correction in the magnitude of the friction drag taking into account the inclination of the plate to the flow, or in the more general case the curvature.

The force Y_R shall be neglected in what follows as it is very small in comparison with the other components that determine the total lift force of the planing bottom.

After adding all the forces exerted on area $S = lb$ by the water, it may be said that the resistance of the plate is composed of the hydrostatic resistance X_F, the form drag X_N, and the friction drag X_R:

$$X = X_F + X_N + X_R \tag{30}$$

and for the components the following expressions are obtained:

$$\left.\begin{aligned} X_F &= -0.5\,\gamma \sin^2 \alpha\,(2b_0 - b)\,S \\ X_N &= -\epsilon\,(2 - \epsilon) \sin \alpha \frac{\rho}{2} S V_0^2 \\ X_R &= -C_f\,(1 - \epsilon)^2 \cos \alpha \frac{\rho}{2} S V_0^2 \end{aligned}\right\} \tag{31}$$

In deriving the resistance forces and in passing from two-dimensional to three-dimensional flow, that is, to a plate of finite span l, the induced drag due to the vortices shed at the surface of the plate, was not introduced.

This drag could be introduced, if by analogy with the airfoil theory, π-shaped vortices are assumed and if the Biot-Savart theorem is considered as applicable without any changes to the present case of motion on the surface separating two fluid mediums.

This assumption may be considered superfluous, because in order that the formulas developed here may be practically applied it is necessary to know the value of the factor ϵ for the given aspect ratio of the plate and the angle of attack. The angle of attack is obtained on the basis of test data and therefore already takes into account the induced drag. It would be incorrect to introduce a second induced drag.

The lift force of a planing plate is expressed as the sum of the hydrostatic lift Y_F, the hydrodynamic lift due to form Y_N, and the lift due to the circulation Y_J:

$$Y = Y_F + Y_N + Y_J \tag{32}$$

where the components are given by the equations

$$\left.\begin{aligned} Y_F &= 0.25\,\gamma \sin 2\alpha\,(2b_0 - b)\,S \\ Y_N &= \left[\epsilon\,(2 - \epsilon)\cos\alpha - 2\,(\cos\alpha + \epsilon - 1)\right]\frac{\rho}{2}\,SV_0^2 \\ Y_J &= 2\,(\cos\alpha + \epsilon - 1)\,\frac{\rho}{2}\,SV_0^2 \end{aligned}\right\} \qquad (33)$$

In the following discussion, use will be made of the derived formulas in a somewhat different form introducing the nondimensional coefficients C_x, C_R, and C_y where

$$\left.\begin{aligned} C_x &= \epsilon\,(2 - \epsilon)\sin\alpha \\ C_R &= C_f\,(1 - \epsilon)^2\cos\alpha \\ C_y &= \epsilon\,(2 - \epsilon)\cos\alpha \end{aligned}\right\} \qquad (34)$$

Thus,

$$\left.\begin{aligned} X_N &= C_x\,\frac{\rho}{2}\,SV_0^2 \\ X_R &= C_R\,\frac{\rho}{2}\,SV_0^2 \\ Y_N + Y_J &= C_y\,\frac{\rho}{2}\,SV_0^2 \end{aligned}\right\} \qquad (35)$$

3. EVALUATION OF EXPERIMENTAL DATA OF SOTTORF

The formulas derived herein permit the determination of the lift and the drag of a partly submerged plate if ϵ is found and $b/b_0 = \chi$ as functions of the parameters of motion as the velocity, angle of attack, and aspect ratio.

The relation between the ratio ϵ and the velocity, the angle of attack α, and the aspect ratio λ of the wetted area will now be determined. In order to solve this problem theoretically, there is required the analytical determination of the flow, in other words, a knowledge of the complex potential function $w = \varphi + \psi i$. In solving this problem, great mathematical difficulties are encountered. Because the problem of giving formulas suitable for practical use is present and mathematical rigor of this analysis is not pretended, use shall be made of the tests of Sottorf (reference 2) on planing plates for the determination of the dependence of ϵ on α, V_0, and λ.

The tests of Sottorf at the present are the only published experimental data that permit analyzing the phenomenon of the planing of a plate with sufficient completeness. It should be remarked that the tests give a large number of test points for small aspect ratios only. For $2 < \lambda < 5$, the number of test points is very small, and in order to obtain the required curves use must be made of the method of interpolation.

For $\lambda > 5$, there are no test data at all but it was possible to obtain theoretically the fundamental relations for $\lambda = \infty$ and then by extrapolating the test curves it was assumed possible to prolong them to the aspect ratio $\lambda = 10$.

The tests of Sottorf were conducted at the Hamburg towing basin and were made on a plate of constant span (l = 300 mm). For constant lift forces, varying from 4 to 45.2 kilograms, the plate was towed, over a range of velocities from 4 to 9 meters per second, at various angle of attack. The results of the test give for each towing trial the following experimental values:

Y lift force of plate, (kg)

X total resistance of plate, (kg)

α angle of attack, (deg)

V_0 towing velocity, (m/sec)

b_0 wetted ~~width~~ chord in the state of rest, (mm)

b wetted ~~width~~ chord in motion, (mm)

M moment with respect to lower edge of plate, (kg/m)

On the basis of the tests of Sottorf, the derived formulas permit obtaining the magnitude ϵ in two ways: either operating with equation (30) and the test data on the resistance to the motion, or using the same test data and equation (32) referring only to the lift forces. In the total resistance to the motion, there enters the component of the frictional resistance on the x-axis. In computing the resistances the probability of error is not excluded because the frictional resistance contains the coefficient C_f, the formulas for which cannot be considered as sufficiently correct for all regimes of the motion.

The factor ϵ can be determined with a greater degree of accuracy from the data and formulas for lift forces. In this case, the component due to the friction is very small so that the errors in the determination of ϵ will be considerably less than in the first case.

The obtained graphs are not considered final and to supplement and correct them it is necessary to turn to the first case as is permitted by the accumulated experimental data on the planing plate.

Thus, ϵ shall be determined from the equation of the lift forces (32).

With the accuracy inherent to all test results, the magnitude of the hydrostatic lift forces for each towing test is determined by

$$Y_F = 0.25\ \gamma \sin 2\alpha\ (2b_0 - b)\ b \cdot 0.3$$

where for γ the value 1000 kilograms per cubic meter was chosen.

Then, subtracting from the total lift force Y measured in the test the lift Y_F, the difference is obtained, which on the basis of equation (32) is connected with the required magnitude ϵ by the following relation:

$$\epsilon\ (2 - \epsilon) = \frac{2\ (Y - Y_F)}{0.3\ \rho b V_0^2 \cos \alpha}$$

By solving this equation for ϵ, the value of ϵ may be obtained for each towing trial. Thus, for example, for $V = 9.85$ millimeters per second and the load $Y = 22.6$ kilograms the results

shown in figure 12 were obtained. A similar evaluation of all the test data of Sottorf gives a series similar to the curves of ϵ as a function of λ and α for the velocities V_0 and load Y. From these curves, as a general rule, it may be concluded that for a given velocity V and vertical load Y on a plate of constant span l, the ratio ϵ increases with increasing angle of attack and the wetted aspect ratio $\lambda = l/b$.

From these curves, the value of ϵ as a function of the angle of attack can be found for any constant value of the aspect ratio $\lambda = l/b$. The curves of figure 13 give the change of ϵ with the angle of attack α for a constant value of the wetted aspect ratio.

The change in ϵ as a function of the aspect ratio λ for constant angles of attack α is shown in figure 14.

The numerical values for these curves are given in table 1.

The available experimental data permit the following conclusions: The value of ϵ does not depend on the velocity of the planing plate and is a function of the angle of attack α and the wetted aspect ratio λ.

For a given λ, the increase of ϵ with the angle of attack α is represented by a straight line. For a constant angle of attack ϵ increases with increasing λ. The straight line of ϵ against α with increase in the parameter λ (fig. 13) approaches a certain straight line that, it may be assumed, corresponds to an infinitely large aspect ratio ($\lambda = \infty$). In the previous section, it was shown that by computation the obtained formulas give, for the partly submerged plate, a lift force Y_N practically equal to zero. If this assumption, which has not been mathematically proved, is made and, the coefficient of $\frac{\rho}{2} S V_0^2$ in the expression for Y_N (equations (33)) are equated to zero, the following relation between ϵ and the angle of attack is obtained.

$$\epsilon (2 - \epsilon) \cos \alpha - 2 (\cos \alpha + \epsilon - 1) = 0$$

from which is obtained

$$\epsilon \underset{\infty}{=} \sqrt{\frac{2 (1 - \cos \alpha)}{\cos \alpha}} \approx 2 \operatorname{tg} \frac{\alpha}{2} \approx \alpha \qquad (36)$$

The obtained expression gives the relation between ϵ and the angle of attack for infinite span.

The curve of ϵ plotted against α according to equation (36) is given in figure 14. The statement that the straight lines of ϵ against α, with increasing λ, approach asymptotically a certain straight line corresponding to $\lambda = \infty$ is confirmed by the obtained analytical relation in equation (36). It should be noted that this expression was obtained independently of any experimental data and the values of the other forces obtained on its basis for $\lambda = \infty$ do not contradict the physical phenomena, moreover, they confirm the asymptotic approach of the experimental curves to the limiting values corresponding to $\lambda = \infty$.

If the dependence of ϵ on α and ∞ is known, for any given angle of attack and aspect ratio the value of the coefficients C_x, C_y, and C_R/C_f can be determined by use of equation (34) and therefore, the drag and the lift of a plate planing at angle of attack α and aspect ratio λ can be computed.

The curves of the coefficients C_x, C_y, and C_R/C_f plotted against λ for various angles of attack α are given in figures 15 to 17. There are also given the values of these coefficients for an infinitely large aspect ratio, the value of ϵ being determined from equation (36).

In addition to ϵ the magnitude $\chi = b/b_0$ must be known for complete hydrodynamic computation of the planing plate. The knowledge of the magnitude χ makes possible the computation of the hydrostatic forces X_F and Y_F. However, the computation shows that the values of X_F and Y_F, for velocities corresponding to rise on the step and greater, are negligibly small in comparison with the remaining acting forces. For this reason, within the range of velocities considered, it may be assumed that these forces are absent.

The value χ evidently depends on the velocity, the angle of attack, and the aspect ratio. An attempt to obtain this relation on the basis of experimental data did not give positive results. The determination of this relation will be returned to later and in order not to defer the discussion it is recommended that the planing angles of $\alpha = 3 - 4^c$ be used to assume the value $\chi = 1.15$, which of course introduces a certain inaccuracy in the hydrodynamic computation at velocities up to the rise on the step. The errors introduced by this approximation, however, rapidly drop and at the rise on the step entirely vanish.

The determination of the experimental relation between the center of pressure and the parameters that determine the motion of the plate are now considered. Here, as before, use is made of the tests of Sottorf. The following results are obtained on the basis of an analysis of these tests.

The forces acting on the partly submerged plate may be divided, as regards the determination of their moments, into the following three kinds:

(1) the friction forces, directed tangentially to the plate whose moment about the lower wetted edge is zero;

(2) the hydrostatic pressure forces, perpendicular to the plate, whose value over an element of the plate db varies linearly. The center of pressure of the sum of the hydrostatic forces is easily determined and their moment about the lower wetted edge of the plate is

$$M_F = \gamma l b^2 \sin \alpha \frac{3b_0 - 2b}{6} \tag{37}$$

(3) the force of the hydrodynamic pressure of the fluid on the plate. These forces, being perpendicular to the plate, give about the lower wetted edge the moment M_N, which is expressed by the following relation:

$$M_N = \int pdb \cdot b = \rho \frac{V_0^2}{2} l \int_0^b \epsilon (2 - \epsilon) bdb \tag{38}$$

This expression was obtained in the following manner. The hydrodynamic force acting on element db will be equal to:

$$dP = \rho \frac{V_0^2}{2} \epsilon (2 - \epsilon) db = \frac{\rho}{2} (V_0^2 - V^2) db$$

Its moment dM_N about the lower wetted edge is given by

$$dM_N = \rho \frac{V_0^2}{2} \epsilon (2 - \epsilon) \, bdb$$

By integrating this expression between the limits 0 to b, equation (38) is obtained for a plate of width l.

It is not difficult to see that the equation for the moment of the hydrodynamic forces about the lower edge of the plate may be briefly expressed in the following form:

$$M_N = \rho \frac{V_0^2}{2} l b^2 C_M \tag{39}$$

where

$$C_M = \frac{1}{b^2} \int_0^b \epsilon (2 - \epsilon) \, bdb \tag{40}$$

It is obvious that the magnitude C_M is a function only of ϵ. This fact is of essential importance in the procedure of evaluating the data of Sottorf, which follows.

From the measured moment of all the forces acting on the planing plate, the moment (computed by means of equation (37)) due to the hydrostatic pressure is subtracted. By dividing the remainder by $\rho \frac{V_0^2}{2} l b^2$, C_M may be obtained. The coefficients C_M computed in this manner for all the test points of Sottorf, determine a certain curve of C_M against ϵ, when graphically presented.

This curve, which with sufficient accuracy is a straight line is shown in figure 18. The straight line, which is computed by the method of least squares, gives the slope $k = 1.58$.

Thus, the relation between the moment coefficient C_M of the hydrodynamic forces and the ratio ϵ may be expressed by the following equation:

$$C_M = k\epsilon = 1.58 \, \epsilon$$

The moment of all the forces acting on the plate about its lower wetted edge may be written in the following form:

$$M = M_F + M_N = \gamma l b^2 \sin \alpha \frac{3b_0 - 2b}{6} + k\epsilon\rho \frac{V_0^2}{2} l b^2 \qquad (42)$$

If for a given velocity and given load the angle of attack of the plate and the wetted aspect ratio are known, the value of ϵ can be found from the curve of ϵ against α and λ. From the obtained equation or from figure 18, the value of the moment coefficient can be found. If required, the center of pressure of the hydrodynamic forces can then be obtained. By adding the moment of the hydrostatic forces obtained from equation (37), the moment of all the forces acting on the plate can also be obtained.

The wetted aspect ratio that is required here may be determined in the following manner. From the data the load coefficient C_B is obtained

$$C_B = \frac{C_y}{\lambda} = \frac{Y}{\frac{\rho}{2} l^2 V^2} \qquad (43)$$

This coefficient characterizes the degree of loading of the plate. On the curve of figure 19 for a given angle of attack and constant C_B, the aspect ratio λ, at which the given plate will plane for the velocity V, width l, and load Y may be found.

In the following discussion, the ratio of the lift force of the plate to the total resistance as the planing efficiency of the plate will be

$$k = \frac{Y}{X}$$

The value of the coefficient k for the case of motion of a plate of finite aspect ratio in a real viscous fluid will now be considered in more detail. The magnitude $1/k = \mu$, the reciprocal of the efficiency, will now be analyzed.

The derived equations permit writing the following expression for μ:

$$\mu = \frac{X}{Y} = \frac{X_F + X_N + X_R}{Y_F + Y_N + Y_J} = \frac{X_F + X_N}{Y_F + Y_N + Y_J} + \frac{X_R}{Y_F + Y_N + Y_J} \qquad (44)$$

The right side of the equation, is expressed by two terms, which permits considering each term separately. The first component term determines the efficiency of the plate of any span for motion in an ideal nonviscous fluid. This magnitude is exactly equal to $\tan \alpha$ because in an ideal fluid the plate is acted on only by normal forces:

$$\frac{X_F + X_N}{Y_F + Y_N + Y_J} = \text{tg } \alpha$$

The second term

$$\frac{X_R}{Y_F + Y_N + Y_J}$$

gives the correction due to the viscosity and, hence, the existence of surface friction. First of all, the term Y_F in the denominator of the expression entering as a lift force due to the hydrodynamic pressure on the wetted plate is rejected because the term Y_F rapidly decreases with increasing velocity and may be already practically neglected starting at velocities equal to 75 percent of the velocity in rising on the step. By neglecting this term, that is considering the plate in the state of planing where its water displacement is negligible, the values for X_R, Y_N, and Y_J determined by equations (35) may be substituted. Then dividing by $\frac{\rho}{2} SV_0^2 \cos \alpha$ there results

$$\frac{X_R}{Y_N + Y_J} = \frac{C_f (1 - \epsilon)^2}{\epsilon (2 - \epsilon)} = \frac{C_f}{\epsilon (2 - \epsilon)} - C_f$$

Thus, μ is given by

$$\mu = \operatorname{tg} \alpha + \frac{C_f (1 - \epsilon)}{\epsilon (2 - \epsilon)} \tag{45}$$

The variation of μ with the angle of attack and aspect ratio of the plate will now be considered. The family of curves (fig. 20) gives the relations obtained by equation (45). The friction coefficient C_f, which as been previously shown, depends on the Reynolds number in the general case, here assumes a constant value equal to 0.003, which corresponds in the case of the turbulent regime to the Reynolds number $Re = 9 \cdot 10^6$. The change of the magnitude μ with the Reynolds number will subsequently be considered. Inspection of the curves for $C_f = 0.003$ permits drawing the following conclusions:

For a constant coefficient of friction and a constant aspect ratio, the value of μ has a sharply defined minimum for a certain angle of attack.

For relatively small deviations from the optimum angle, the impairment of the planing efficiency of the plate, that is the increase in the magnitude μ, will be considerable.

For the friction coefficient $C_f = 0.003$, the most favorable angle of attack lies in the range of 4° to 2°. With increasing aspect ratio, the most favorable angle of attack decreases from 4° at $\lambda = 0.5$ to 2° at $\lambda = \infty$.

The largest value of the planing efficiency is attained for an infinitely large aspect ratio ($\lambda = \infty$). It may be assumed, however, that the efficiency for aspect ratio $\lambda \cong 10$ already differs only slightly from the value of the efficiency at $\lambda = \infty$. Thus, for $\lambda = 10$, $\mu = 0.078$; whereas for $\lambda = \infty$, $\mu = 0.0755$, that is for the aspect ratio $\lambda = 10$ the efficiency is less than that for $\lambda = \infty$ by only 3 percent.

Because the analytical part of this paper does not fully take into account all the factors that impair the planing efficiency of the plate, it may be expected that an aspect ratio of 7:8 will be the most favorable. Beyond this limiting value there may be expected not an improvement, but an impairment of the planing efficiency as a result of separation of the flow and the turbulence, which have not been considered here.

The computation of the resistance (fig. 23) with increasing velocity for plates planing at constant load $Y = 18$ kilograms and constant angle of attack $\alpha = 4^{\circ}$ shows that even with account taken only of the surface friction there is for a certain aspect ratio a limiting optimum value of the efficiency k and further increase in the aspect ratio impairs the efficiency (fig. 21). Thus, in the case of the turbulent flow this value is $\lambda = 7.5$ and in the case of transition to the turbulent flow the optimum value is $\lambda = 9.7$.

The reason for the impairment of the planing efficiency after reaching certain values of λ is to be found in the increasing resistance due to the surface friction for a constant value of the hydrodynamic resistance $X_N = Y \tan \alpha$. In the process of planing, the frictional resistance is influenced by the following factors. With increasing velocity, the Reynolds number drops and approaches a constant value that for a turbulent regime gives an increase in the coefficient of friction (a factor that increases the frictional resistance). With increasing velocity there is a decrease in the friction surface area (a factor that decreases the frictional resistance). Because the frictional resistance is proportional to the square of the velocity, the increase in the friction due to the increase in velocity is so large that it compensates the drop in the resistance due to the decreased friction area and together with the added resistance due to the change of the Reynolds number gives as a final result an increase in the friction.

The dependence of μ on the angle of attack and the aspect ratio for $C_f = 0.003$ are shown in figure 20. Now it will be shown how the optimum values of the angle of attack and the values of μ change as C_f changes.

The minimum values of μ as functions of the optimum angle of attack for three different coefficients of friction C_f equal to 0.0025, 0.003, and 0.004 are plotted in figure 22.

The values of the optimum angle and the values of k, the efficiency of the plate, are laid off on the ordinate. Two groups of curves determine the change in the optimum angle of attack and efficiency k for the three values of C_f, 0.0025, 0.003, and 0.004. The dotted curves refer to the same aspect ratio. On the abscissa are laid off the values of the load coefficients denoted by

$$C_B = \frac{C_y}{\lambda} = \frac{Y}{\frac{\rho}{2} l^2 V^2}$$

Inspection of these curves permits drawing the following conclusions:

With increasing Reynolds number, which in the case of turbulent motion always corresponds to a decrease in the friction coefficient C_f, the planing efficiency of the plate improves. At the same time there is also a decrease in the optimum angle of attack.

For sufficiently small load coefficients (which correspond to aspect ratios λ from 7 to 10), the planing efficiency differs little from the value for infinite span. In accordance with what has been said, for load coefficients $C_B < 0.01$ there must be expected not an increase in the efficiency but a decrease due to the hydrodynamic resistance, which was not taken into account, as well as the frictional resistance.

The change in the separate resistance terms the sum of which is the total resistance of the plate, will now be considered. The computation for a plate of width $l = 0.3$ meter has here been carried out assuming the angle of attack constant and equal to 4° and choosing the velocities over the range 0 to 22 meters per second. The vertical load was taken constant and equal to 18 kilograms. The most accurate results, as has been shown, are to be expected at velocities of pure planing. Here the curves shown in figure 23 are obtained. The hydrostatic resistance rapidly increases from zero to the maximum value that corresponds to the velocity $V = 2$ meters per second, then rapidly drops and at $V = 10$ meters per second is practically equal to zero, that is, it may be assumed that for velocities above $V = 10$ meters per second pure planing occurs.

The form drag, increasing from zero, reaches at the velocity $V = 10$ meters per second its maximum value $X_N = 18 \tan 4^\circ$ and practically remains constant with further increase in velocity.

In computing the resistance due to the surface friction, two regimes are assumed. The first regime is the gradual transition of the flow from laminar to turbulent and it corresponds to the curve X_{RL}. The second regime is that of complete turbulent flow, this case corresponds to the curve X_{RT}. As was to have been expected, the turbulent regime gives an increased surface friction. The general conclusion with regard to the frictional resistance is the following: At a certain velocity ($V = 6$ m/sec) the frictional resistance, starting from zero, reaches a maximum value, then drops, having minimums at $V = 15$ and 17.5 meters per second for the

laminar and turbulent states, respectively, and with further increase in velocity slowly increases. In analyzing the change in the planing efficiency, the reasons for this phenomenon have been considered.

The total curve of the resistance in the case of the turbulent regime gives the following character of the flow: At the velocity $V = 6$ meters per second, which is termed the critical velocity, the curve has a maximum resistance. Then at $V = 15$ meters per second the curve has a minimum, thereafter it slowly increases due to the increasing frictional resistance. An analogous character of the flow is also possessed by the resistance curve for the case of transition from laminar to turbulent flow.

In conclusion, the results of computation with the formulas and curves given in this paper are compared with the data obtained directly from tests. This comparison was made for three cases. The first two refer to the test data of Sottorf on a plate with $l = 0.3$ meter. In the first case the plate, being loaded by a vertical force A equal to 8 kilograms, was towed with velocity V equal to 4 meters per second; in the second case, the same plate had the load $A = 18$ kilograms and the corresponding velocity was $V = 6$ meters per second. The third case refers to the towing of a seaplane model. The computed and experimental curves obtained for the plate permit drawing the following conclusions:

The results obtained by computation almost coincide with the towing test results (fig. 24). For the same plate towed at two different velocities and loads, there are two corresponding friction regimes; namely, at $V = 4$ meters per second and $A = 8$ kilograms there is a transition from laminar to turbulent flow (equation (26)); whereas at $V = 6$ meters per second and $A = 18$ kilograms the friction has a clearly marked turbulent character.

Figure 25 shows the agreement of the theoretical and towing test results for the seaplane model.

The curve X_T gives the total resistance of the model computed on the assumption of a flat bottom, the angle of attack of the model being taken from the arithmetic mean of the angles with the water line. The curves X_K give the same resistance corrected by approximate formulas for the keel of the model.

Notwithstanding the fact that the plate is only a rough approximation to the bottom of the model, the agreement between the theory and experiment is considered to be very satisfactory.

Translated by S. Reiss
National Advisory Committee
for Aeronautics.

REFERENCES

1. Prandtl, L., and Tietjens, O. G.: Applied Hydro- and Aeromechanics. McGraw-Hill Book Co., Inc., 1934, p. 291.

2. Sottorf, W.: Experiments with Planing Surfaces. NACA TM 661, 1932.

Table 1. - Values of mean relative retardation ϵ as function of angle of attack α and aspect ratio λ.

λ \ α	1	2	3	4	5	6	7	8	9	10
0.5	0.5	1.05	1.60	2.10	2.60	3.15	3.65	4.15	4.70	5.20
1	0.80	1.55	2.25	3.00	3.90	4.50	5.40	6.10	6.90	7.60
1.5	1.00	1.95	2.80	3.80	4.85	5.75	6.85	7.85	8.80	9.75
2	1.15	2.30	3.30	4.40	5.00	6.70	7.95	9.10	10.25	11.30
3	1.40	2.75	4.00	5.40	6.70	8.15	9.45	10.90	12.15	13.10
4	1.50	3.00	4.50	6.00	7.45	9.00	10.50	12.00	13.50	14.95
5	1.60	3.20	4.80	6.35	7.95	9.60	11.15	12.75	14.40	16.00
6	1.65	3.30	4.95	6.60	8.25	9.90	11.55	13.20	14.85	16.50
7	1.695	3.36	5.04	6.72	8.40	10.08	11.75	13.43	15.12	16.80
8	1.70	3.39	5.09	6.78	8.47	10.17	11.87	13.56	15.25	16.95
9	1.705	3.41	5.11	6.82	8.52	10.23	11.94	13.64	15.34	17.05
10	1.71	3.42	5.13	6.84	8.55	10.26	11.97	13.70	15.41	17.10
∞	1.735	3.49	5.23	6.99	8.75	10.50	12.25	14.00	15.80	17.60

Table 2. Values of μ as function of α and λ for $C_f = 0.003$

λ \ α	1	2	3	4	5	6	7	8	9	10
0.5	0.2820	0.1970	0.1650	0.1600	0.1670	0.1785	0.1930	0.2040	0.2200	0.2340
1	0.1950	0.1430	0.1305	0.1334	0.1445	0.1615	0.1725	0.1920	0.2090	0.2260
1.5	0.1670	0.1220	0.1140	0.1195	0.1335	0.1510	0.1635	0.1850	0.2030	0.2220
2	0.1470	0.1080	0.1035	0.1140	0.1285	0.1450	0.1620	0.1810	0.1990	0.2180
2.5	0.1360	0.1010	0.0990	0.1090	0.1240	0.1405	0.1580	0.1760	0.1945	0.2130
3	0.1280	0.0963	0.0945	0.1060	0.1215	0.1380	0.1554	0.1730	0.1910	0.2100
3.5	0.1210	0.0926	0.0926	0.1035	0.1185	0.1350	0.1525	0.1710	0.1890	0.2080
4	0.1180	0.0905	0.0900	0.1015	0.1160	0.1327	0.1500	0.1680	0.1870	0.2050
4.5	0.1145	0.0885	0.0887	0.1000	0.1147	0.1310	0.1480	0.1660	0.1840	0.2020
5	0.1120	0.0855	0.0870	0.0990	0.1125	0.1295	0.1460	0.1645	0.1825	0.2010
6	0.1080	0.0835	0.0855	0.0975	0.1115	0.1270	0.1440	0.1620	0.1800	0.1980
7	0.1060	0.0820	0.0840	0.0960	0.1100	0.1250	0.1410	0.1590	0.1780	0.1960
8	0.1036	0.0805	3.0837	0.0950	0.1090	0.1240	0.1405	0.1580	0.1760	0.1940
9	0.1020	0.0795	0.0820	0.0940	0.1055	0.1230	0.1390	0.1560	0.1740	0.1920
10	0.1010	0.0785	0.0805	0.0925	0.1040	0.1220	0.1380	0.1550	0.1730	0.1900
∞	0.1010	0.0760	0.0780	0.0890	0.1025	0.1165	0.1320	0.1490	0.1650	0.1820

Table 3. Values of μ as function of α and λ for $C_f = 0.004$

λ \ α	1	2	3	4	5	6	7	8	9	10
0.5	.65	0.2520	0.1960	0.1830	0.1850	0.1940	0.2060	0.2180	0.2315	0.2450
1	.25 0	0.1750	0.1530	0.1490	0.1570	0.1700	0.1840	0.2050	0.2170	0.2330
1.5	0.	0.1445	0.1 05	0.1310	0.1430	0.1570	0.1730	0.1900	0.2070	0.2260
2	0.1910	0.1285	0.1190	0.1230	0.1350	0.1500	0.1670	0.1840	0.2030	0.2200
3	0.1640	0.1140	0.1060	0.1140	0.1270	0.1430	0.1590	0.1760	0.1950	0.2140
4	0.1490	0.1070	0.1000	0.1090	0.1220	0.1370	0.1540	0.1715	0.1900	0.2070
5	0.1420	0.1030	0.0985	0.1060	0.1200	0.1340	0.1510	0.1680	0.1860	0.2040
6	0.1380	0.1000	0.0955	0.1040	0.1180	0.1330	0.1500	0.1660	0.1840	0.2010
7	0.1350	0.0980	0.0935	0.1020	0.1160	0.1310	0.1480	0.1640	0.1820	0.1990
8	0.1335	0.0950	0.0920	0.1000	0.1140	0.1290	0 1450	0.1620	0.1800	0.1970
9	0.1320	0.0935	0.0895	0.0990	0.1125	0.1270	0.1440	0.1600	0.1780	0.1960
10	0.1310	0.0920	0.0885	0.0970	0.1105	0.1250	0.1420	0.1590	0.1765	0.1940
∞	0.1290	0.0890	0.0876	0.0945	0.1060	0.1210	0.1360	0.1520	0.1690	0.0559

Table 4. Values of μ as function of α and λ for $C_f = 0.0025$

λ \ α	1	2	3	4	5	6	7	8	9	10
0.5	0.2380	0.1750	0.1480	0.1490	0.1570	0.1700	0.1850	0.2010	0.2170	0.2310
1	0.1650	0.1260	0.1200	0.1260	0.1390	0.1550	0.1710	0.1870	0.2060	0.2230
1.5	0.1440	0.1070	0.1030	0.1140	0.1290	0.1460	0.1640	0.1810	0.1990	0.2170
2	0.1340	0.1000	0.0970	0.1080	0.1240	0.1400	0.1590	0.1760	0.1940	0.2120
3	0.1100	0.0870	0.0900	0.1030	0.1180	0.1350	0.1530	0.1700	0.1890	0.2080
4	0.1010	0.0814	0.0851	0.0980	0.1140	0.1300	0.1480	0.1660	0.1850	0.2030
5	0.0963	0.0785	0.0820	0.0945	0.1100	0.1270	0.1450	0.1630	0.1820	0.2000
6	0.0936	0.0765	.0800	0.0930	0.1085	0.1250	0.1430	0.1610	0.1790	0.1980
7	0.0 12	0.0735	0.0785	0.0915	0.1070	0.1235	0.1405	0.1590	0.1770	0.1950
8	0.0900	0.0720	0.0770	0.0900	0.1055	0. 220	0.1390	0.1580	0.1750	0.1925
9	0.0899	0.0710	0.0760	0.0890	0.1040	0.1210	0.1380	0.1560	0.1740	0.1910
10	0.0875	0.0700	0.0745	0.0870	0.1025	0.1190	0.1370	0.1540	0.1720	0.1900
∞	0.0860	0.0690	0.0725	0.0830	5.0961	0.1130	0.1300	0.1475	0.1640	0.1810

Table 5. Optimum values of k and α as functions of the friction coefficient C_f

λ	$C_f = 0{,}0025$			$C_f = 0{,}003$			$C_f = 0{,}0$		
	k	α	$\frac{C_y}{\lambda}$	k	α	$\frac{C_y}{\lambda}$	k	α	$\frac{C_y}{\lambda}$
0.5	6.80	3°31′	0.0715	6.30	3°49′	0.0780	6.00	4°03′	0.0870
1	8.45	3°01′	0.0445	7.50	3°21′	0.0490	6.65	3°42′	0.0560
1.5	9.35	2°46′	0.0360	8.75	3°03′	0.0380	7.65	3°25′	0.0435
2	10.45	2°33′	0.0280	9.70	2°49′	0.0295	8.40	3°12′	0.0350
3	11.45	2°25′	0.0220	10.85	2°36′	0.0215	9.40	2°57′	0.0260
4	12.30	2°20′	0.0170	11.45	2°33′	0.0175	9.85	2°52′	0.0210
5	12.90	2°17′	0.0140	11.95	2°29′	0.0145	10 45	2°46′	0.0170
6	13.40	2°15′	0.0120	12.40	2°27′	0.0120	10.75	2°43′	0.0145
7	13.70	2°15′	0.0110	12.60	2°26′	0.0110	11.00	2°41′	0 0125
8	13.90	2°15′	0.0100	12.75	2°25′	0.01050	11.25	2°40′	0.0110
9	14.10	2 14′	0.0099	12.85	2°25′	0.0100	11.35	2°39′	0.0100
10	14.30	2°14′	0.0095	12.90	2°2.′	0.0095	11.60	2°38′	0.0095

Table 6. Values of form drag coefficient C_X as function of α and λ

λ \ α	1	2	3	4	5	6	7	8	9	10
0.5	0.00020	0.00070	0.0016	0.0029	0.0045	0.0064	0.0087	0.0116	0.0143	0.0177
1	0.00030	0.00110	0.0023	0.0042	0.0066	0.0094	0.0126	0.0168	0.0210	0.0256
2.5	0.00035	0.00140	0.0030	0.0054	0.0083	0.0120	0.0160	0.0212	0.0265	0.0325
2	0.00040	0.00160	0.0035	0.0062	0.0098	0.0140	0.0186	0.0246	0.0308	0.0376
3	0.00045	0.00190	0.0041	0.0074	0.0115	0.0165	0.0222	0.0292	0.0363	0.0444
4	0.00047	0.00210	0.0046	0.0082	0.0126	0.0182	0.0243	0.0320	0.0397	0.0484
5	0.00052	0.00220	0.0048	0.0086	0.0134	0.0192	0.0256	0.0337	0.0417	0.0510
6	0.00055	0.00230	0.0050	0.0089	0.0138	0.0198	0.0264	0.0345	0.0429	0.0526
7	0.00057	0.00230	0.0051	0.0090	0.0140	0.0200	0.0268	0.0350	0.0436	0.0536
8	0.00058	0.00230	0.0052	0.0091	0.0141	0.0202	0.0271	0.0352	0.0440	0.0540
9	0.00058	0.00235	0.0052	0.0092	0.0142	0.0203	0.0273	0.0354	0.0443	0.0542
10	0.00059	0.00235	0.0053	0.00922	0.01425	0.0203	0.0274	0.0356	0.0445	0.0544
∞	0.00059	0.00239	0.00535	0.0095	0.0145	0.0203	0.0284	0.0362	0.0456	0.0559

Table 7. Values of lift coefficient $C_y = C_{yN} + C_{yT}$ as function of α and λ

λ \ α	1	2	3	4	5	6	7	8	9	10
0.5	0.0110	0.0193	0.0305	0.0415	0.0515	0.0609	0.0708	0.0820	0.0904	0.1050
1	0.0165	0.0300	0.0450	0.0601	0.0750	0.0900	0.1026	0.1210	0.1330	0.1505
1.5	0.0205	0.0385	0.0560	0.0745	0.0950	0.1142	0.1300	0.1515	0.1680	0.1900
2	0.0232	0.0435	0.0665	0 0860	0.1090	0.1295	0.1510	0.1750	0.1950	0.2150
3	0.0275	0.0520	0.0800	0.1030	0.1300	0.1540	0.1790	0.2055	0.2280	0.2500
4	0.0300	0.0580	0.0880	0.1150	0.1440	0.1700	0.1970	0.2250	0.2500	0.2740
5	0.0320	0.0615	0.0930	0.1230	0.1520	0.1800	0.2090	0.2375	0.2640	0.2890
6	0.0329	0.0640	0.0960	0.1270	0.1570	0.1870	0.2160	0.2450	0.2710	0.2980
7	0.0332	0.0655	0.0980	0.1300	0.1600	0.1913	0.2200	0.2500	0.2760	0.3040
8	0.0332	0.0660	0.0990	0.1310	0.1617	0.1940	0.2230	0.2520	0.2790	0.3070
9	0.0338	0.0670	0.1000	0.1320	0.1625	0.1955	0.2240	0.2535	0.2800	0.3080
10	0.0338	0.0672	0.1000	0.1320	0.1630	0.1960	0.2240	0.2540	0.2810	0.3090
∞	0.0350	0.0685	0.1020	0.1350	0.1670	0.1990	0.2290	0.2590	0.2890	0.3180

Table 8. Values of load coefficient $C_B = C_y/\lambda$ as function of α and λ

λ \ α	1	2	3	4	5	6	7	8	9	10
0.5	0.022	0.0386	0.0610	0.083	0.1030	0.1218	0.1416	0.1640	0.1808	0.2100
1	0.0165	0.0300	0.0450	0.0601	0.0750	0.0900	0.1026	0.1210	0.1330	0.1505
1.5	0.0137	0.0257	0.0374	0.0496	0.0535	0.0763	0.0868	0.1010	0.1120	0.1266
2	0.0116	0.02175	0.03325	0.0430	0.0545	0.06475	0.0755	0.0875	0.0975	0.1075
3	0.00918	0.0173	0.0267	0.0344	0.0434	0.0513	0.0597	0.0685	0.0760	0.0834
4	0.0075	0.0145	0.0220	0.0284	0.0360	0.0425	0.0493	0.0563	0.0625	0.0686
5	0.0064	0.0123	0.0186	0 0246	0.0304	0.0360	0.0418	0.0475	0.0528	0.0578
6	0.00548	0.01066	0.0160	0.0212	0.0262	0.0312	0.0360	0.0408	0.0452	0.0497
7	0.00475	0.00935	0.0140	0.0186	0.0228	0.0274	0.0314	0.0357	0.0394	0.0435
8	0.00415	0.00825	0.0124	0.0164	0.0202	0.02425	0.0279	0.0315	0.0349	0.0384
9	0.00375	0.00745	0.0111	0.0147	0.0181	0.0217	0.0249	0.0282	0.03106	0.0342
10	0.00338	0.00672	0.0100	0.0132	0.0163	0.0196	0.0224	0.0254	0.0281	0.0309

Table 9. Values of ratio C_R/Cf as a function of α and λ

α	1	2	3	4	5	6	7	8	9	10
0.5	0.992	0.980	0.970	0.960	0.946	0.935	0.920	0.910	0.898	0.884
1	0.986	0.970	0.956	0.940	0.923	0.908	0.888	0.874	0.854	0.840
1.5	0.982	0.963	0.944	0.924	0.903	0.886	0.862	0.844	0.821	0.804
2	0.978	0.956	0.934	0.912	0.888	0.866	0.840	0.822	0.795	0.776
3	0.974	0.946	0.920	0.894	0.868	0.840	0.812	0.788	0.761	0.736
4	0.971	0.939	0.911	0.884	0.855	0.824	0.794	0.767	0.739	0.710
5	0 968	0.935	0.905	0.876	0.846	0.813	0.783	0.754	0.725	0.695
6	0.966	0.933	0.902	0.870	0.840	0.806	0.776	0.746	0.715	0.686
7	0.960	0.931	0.900	0.868	0.837	0.802	0.771	0.742	0.709	0.681
8	0.9655	0.930	0.899	0.866	0.834	0.801	0.768	0.740	0.706	0.679
9	0.965	0.930	0.899	0.865	0.833	0.800	0.767	0.738	0 705	0.677
10	0.964	0.930	0.899	0.864	0.832	0.800	0.766	0.737	0.705	0.675
∞	0.960	0.930	0.900	0.863	0.830	0.800	0.770	0.740	0.710	0.680

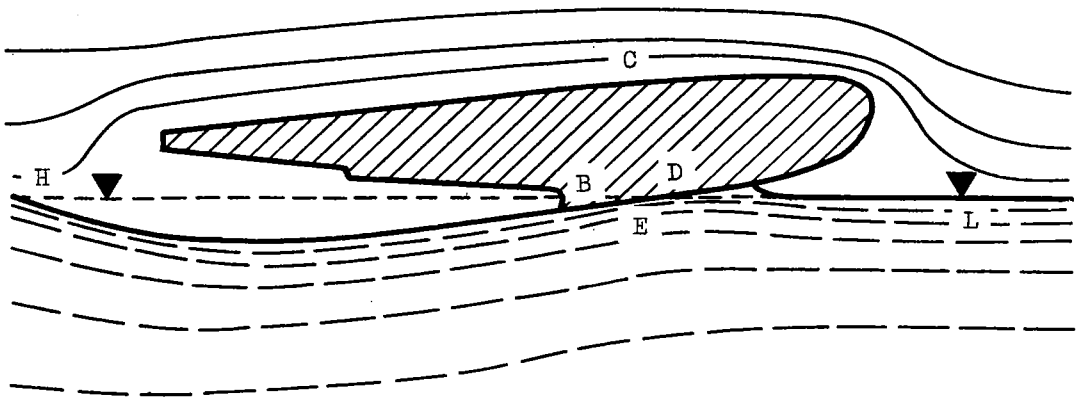

Figure 1. - Flow about seaplane float in two-dimensional flow.

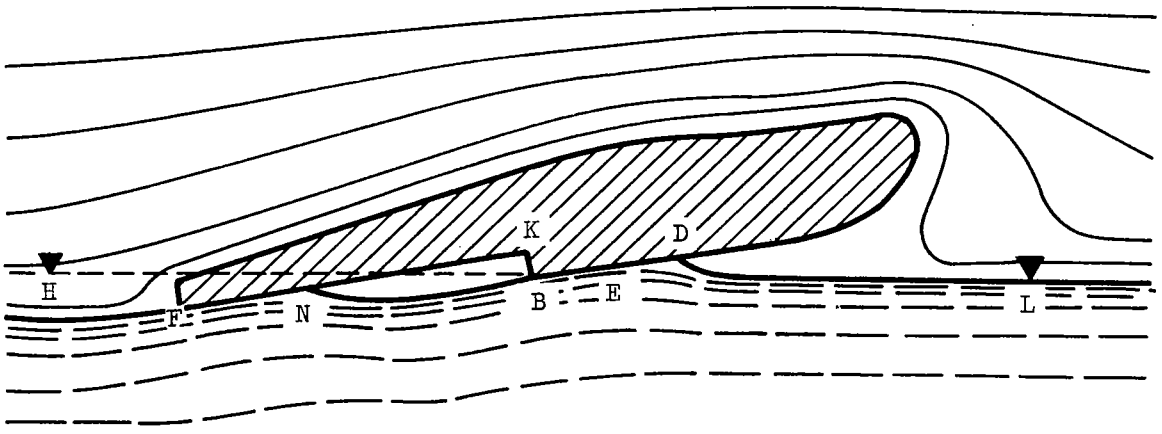

Figure 2. - Flow about flying-boat-hull bottom in two-dimensional flow.

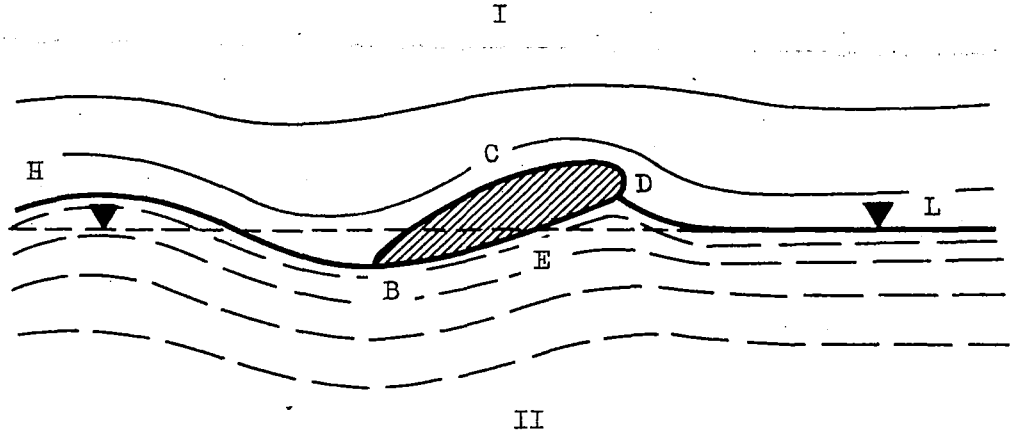

Figure 3.

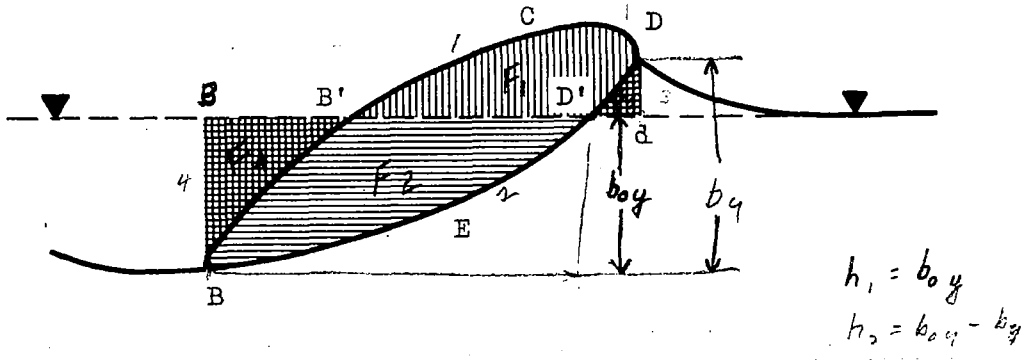

Figure 4.

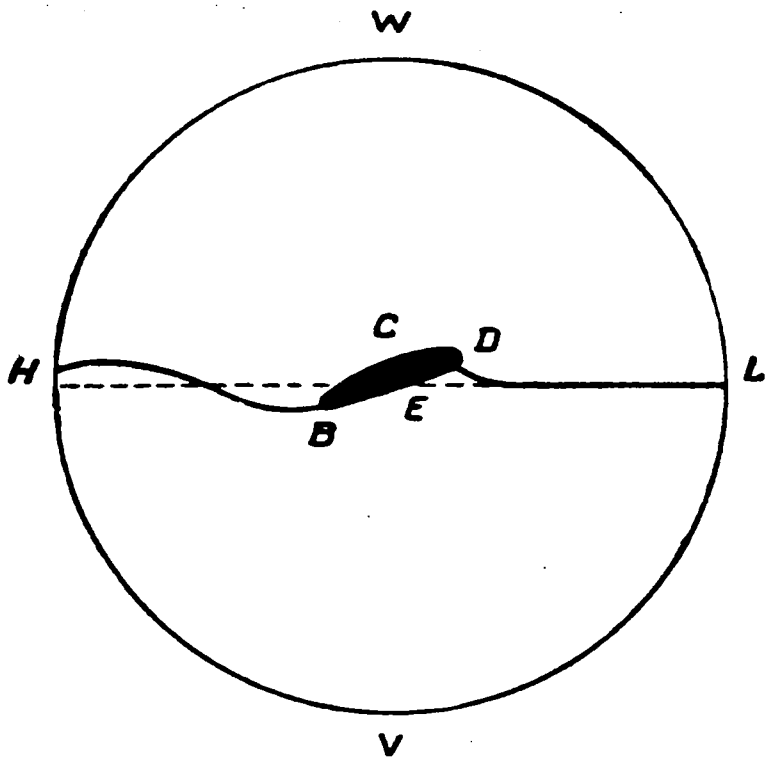

Figure 5.

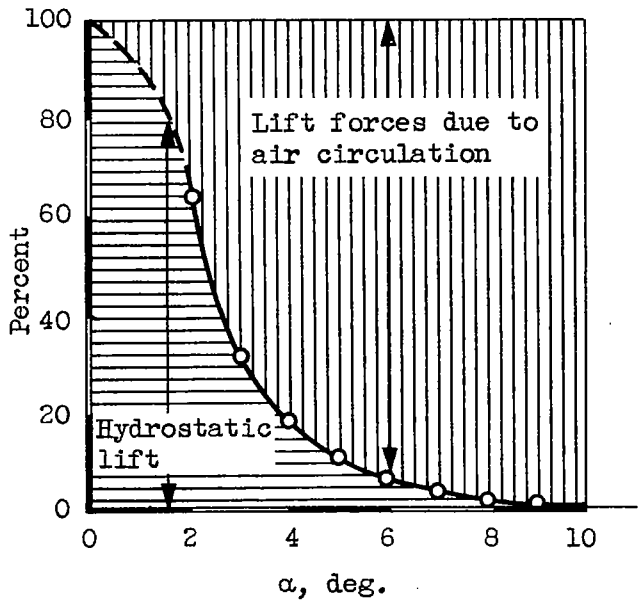

Figure 6. - Variation of hydrostatic and hydrodynamic lift forces expressed in percentage of sum with angle of attack for planing plate at V = 6 meters per second, load Y = 18 kilograms, and width λ = 0.3 meter.

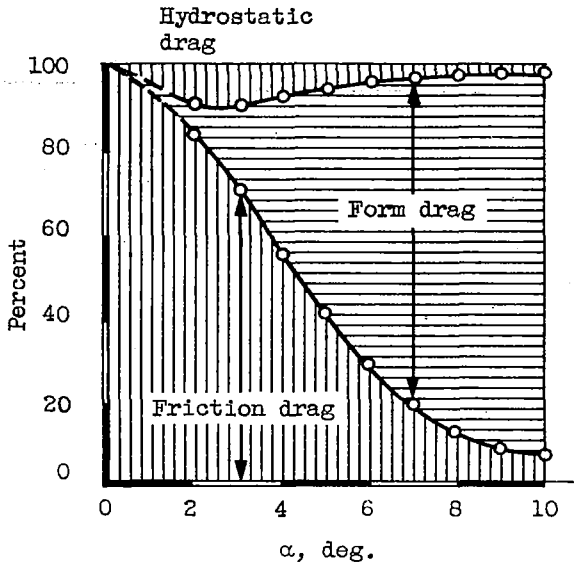

Figure 7. - Variation of friction and form resistances expressed in percentage of sum with angle of attack for a flat-plate planing at V = 6 meters per second, load Y = 18 kilograms, and width l = 0.3 meter.

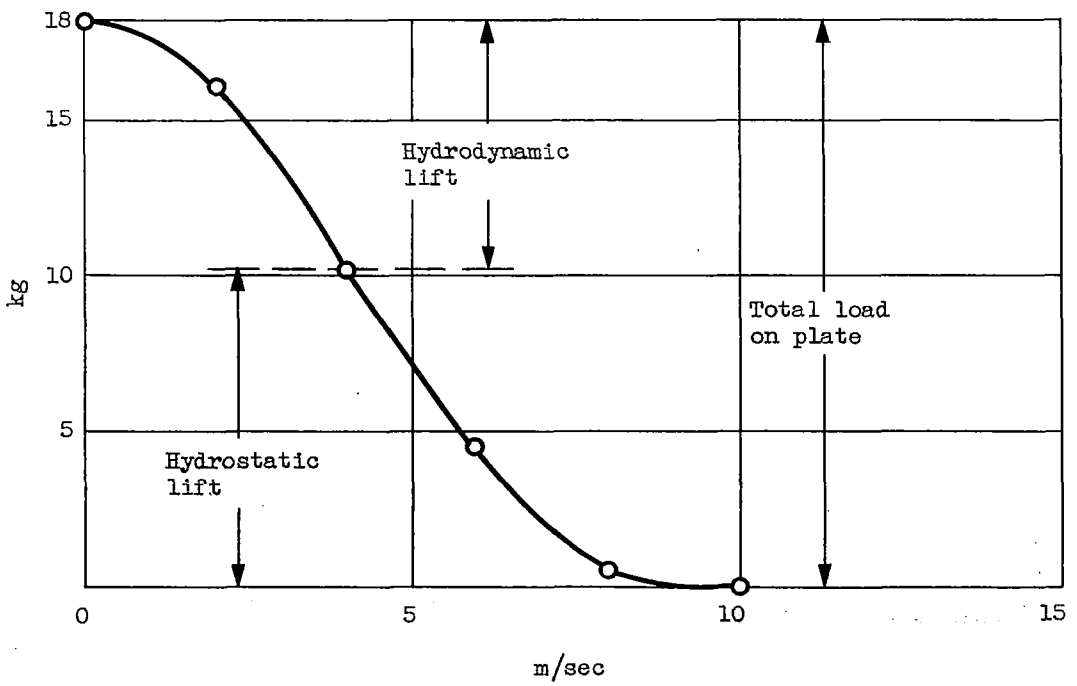

Figure 8. - Curve of relation between hydrostatic and hydrodynamic lift forces computed for plate planing at angle of attack $\alpha = 4^{\circ}$ and load Y = 18 kilograms.

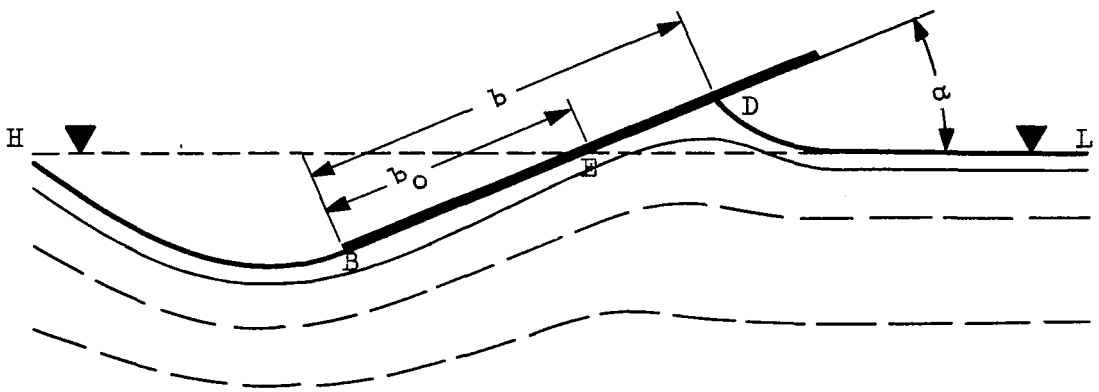

Figure 9. - Motion of planing flat plate.

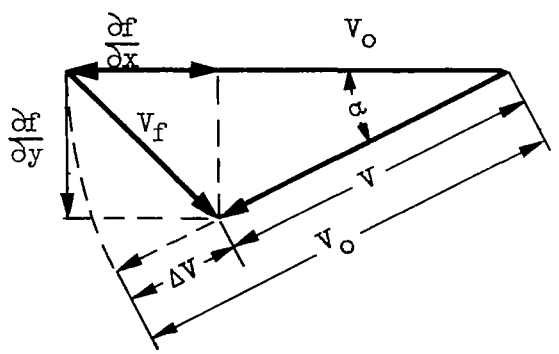

Figure 10.

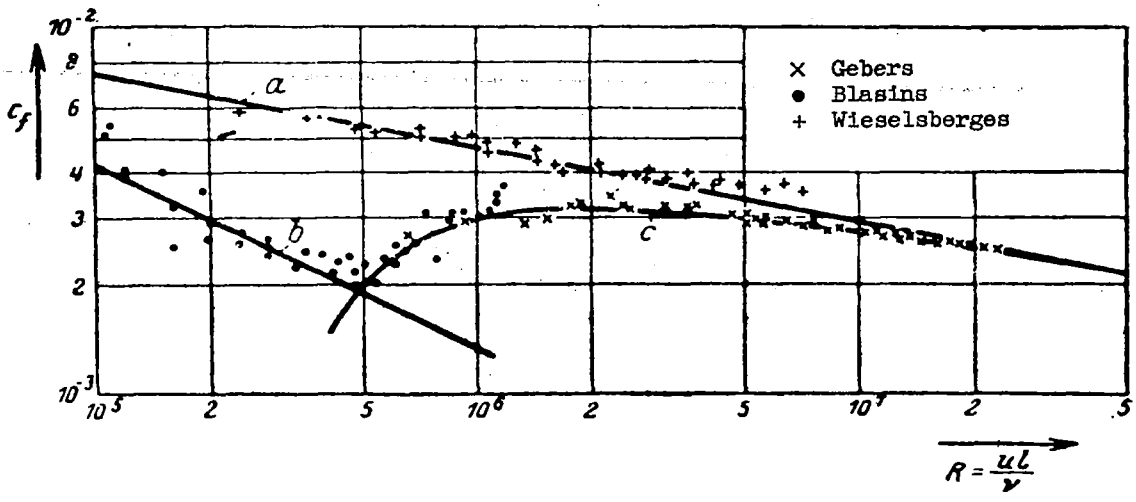

Figure 11. - Dependence of friction coefficient on Reynolds number for flat plates.

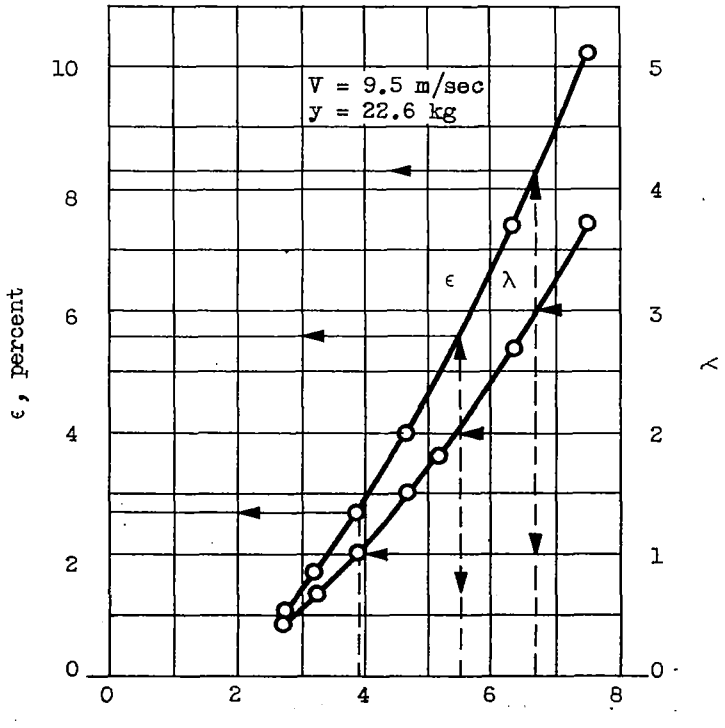

Figure 12.

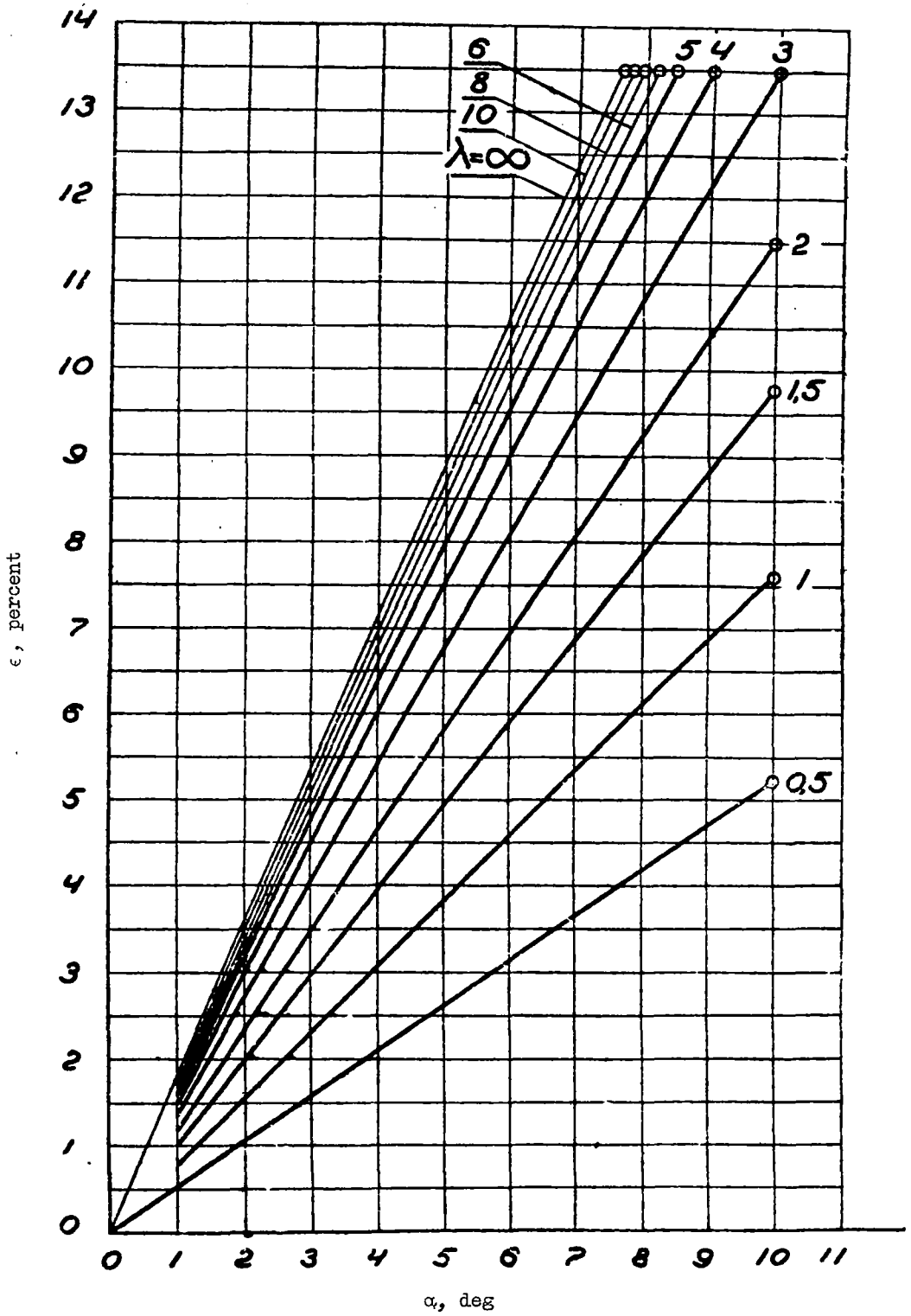

Figure 13. - Dependence of ϵ on α and λ.

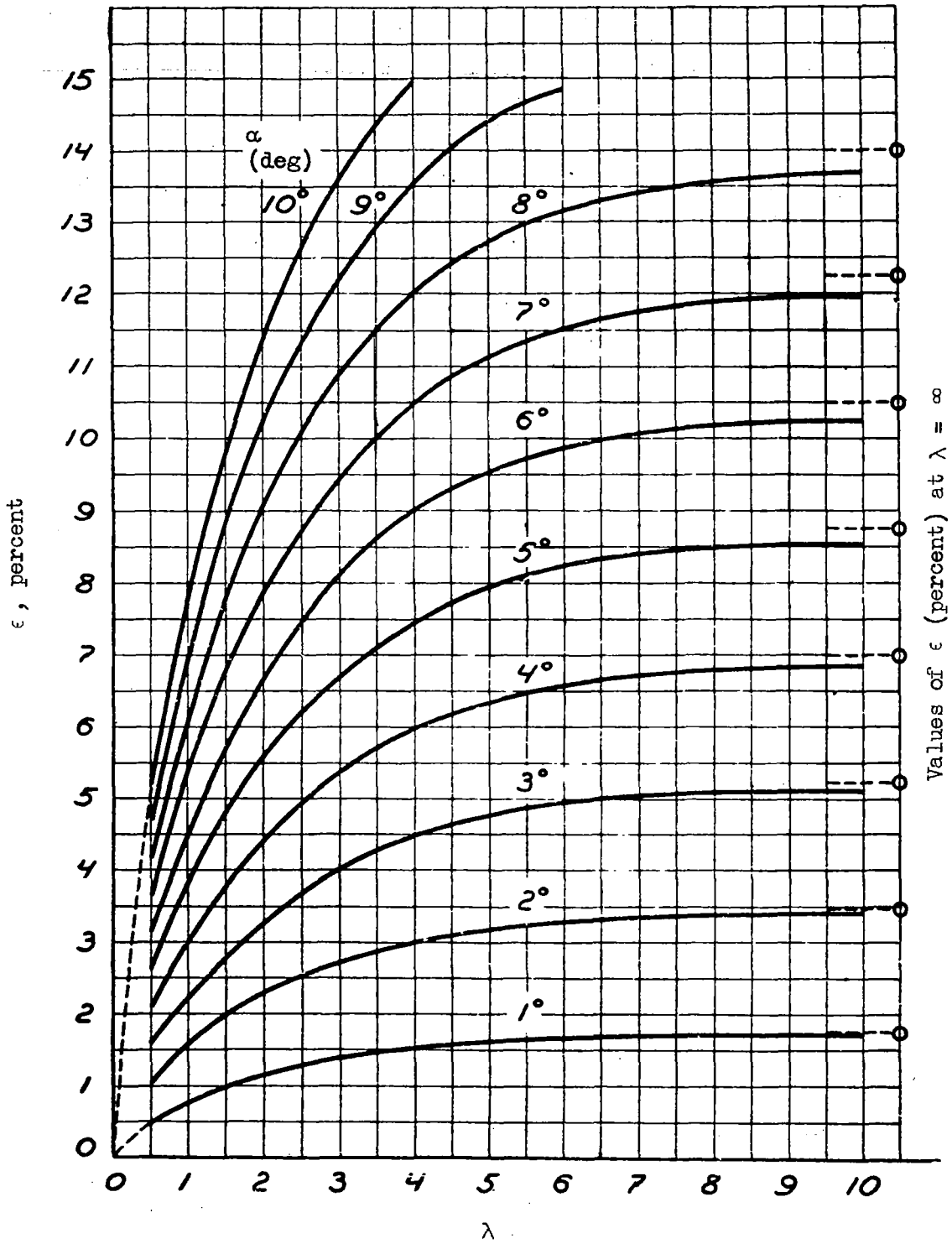

Figure 14. - Dependence of ϵ on λ and α.

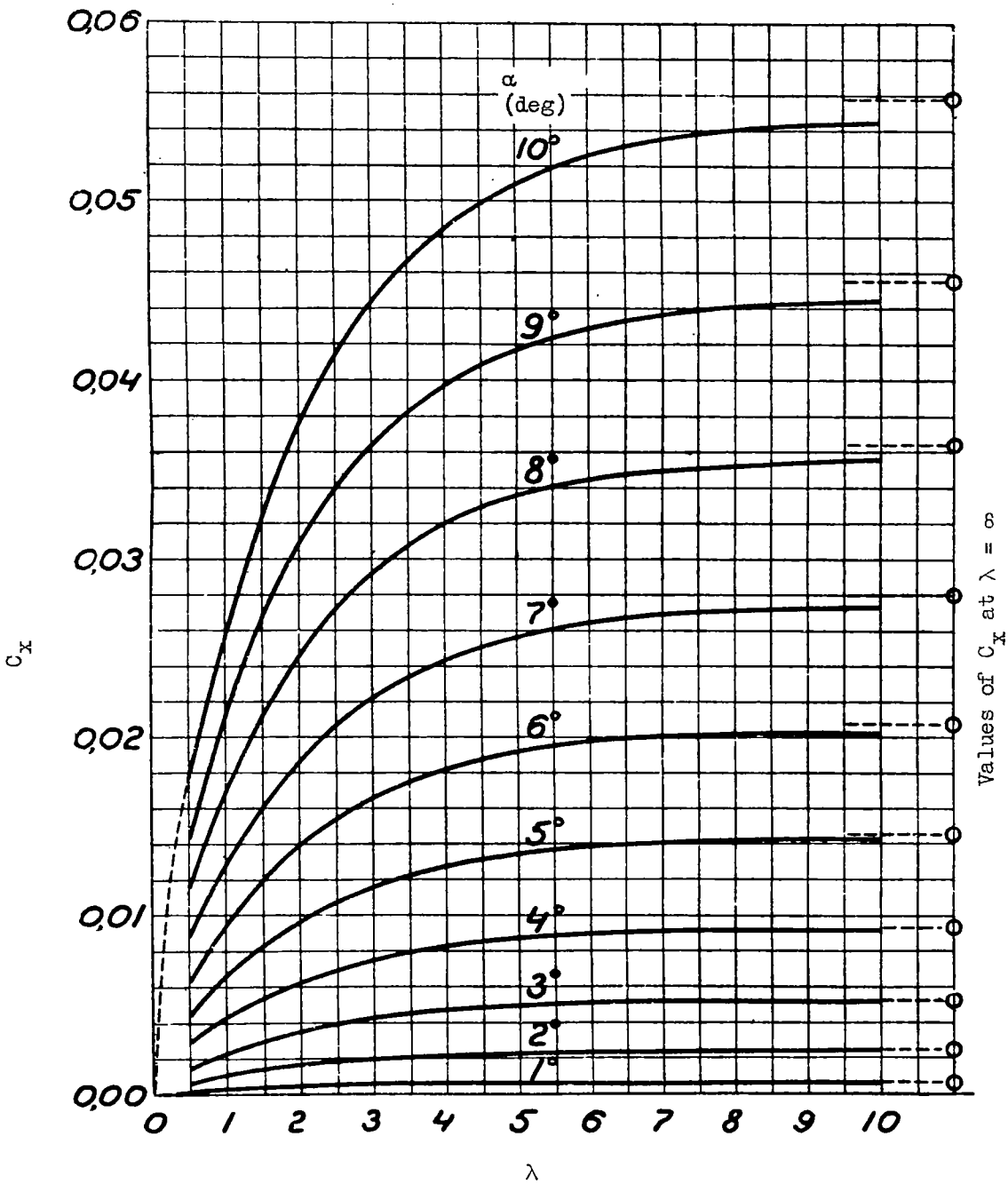

Figure 15. - Dependence of form drag coefficient on α and λ.

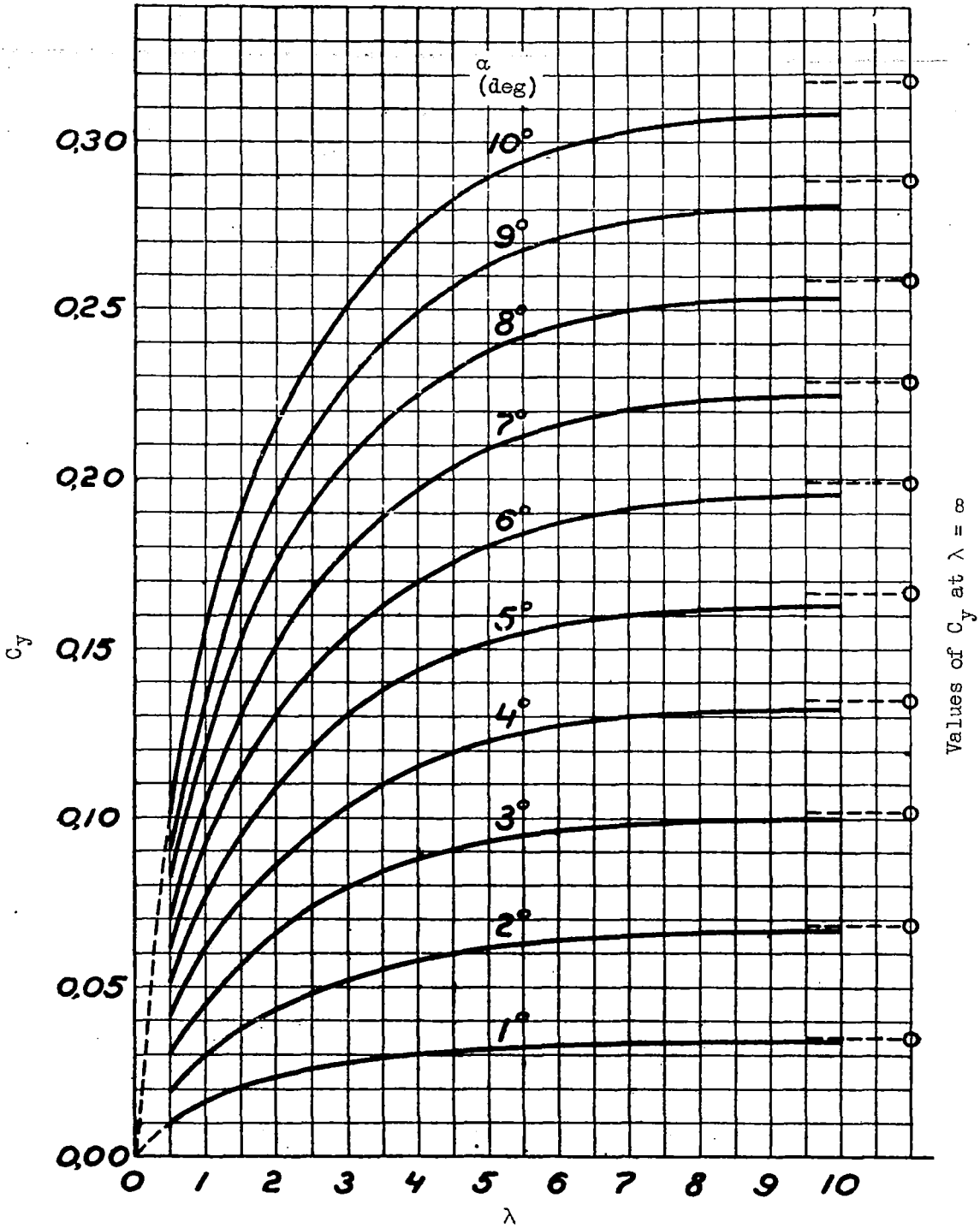

Figure 16. - Dependence of lift force $C_y = C_{y^N} + C_{y^J}$ on angle of attack α and aspect ratio λ.

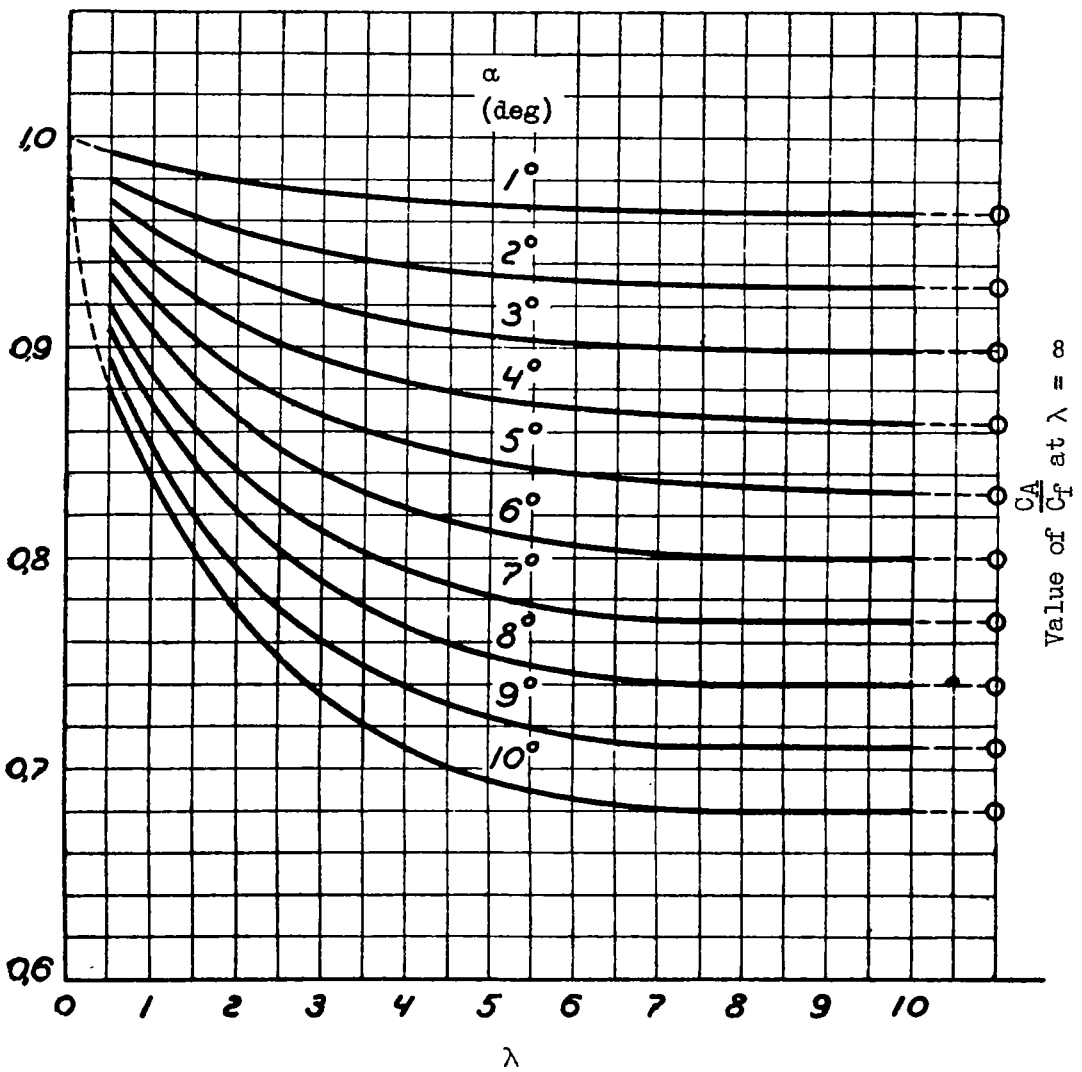

Figure 17. - Dependence of ratio $C_R/C_f = (1 - \epsilon)^2 \cos \alpha$ on angle of attack α and aspect ratio λ.

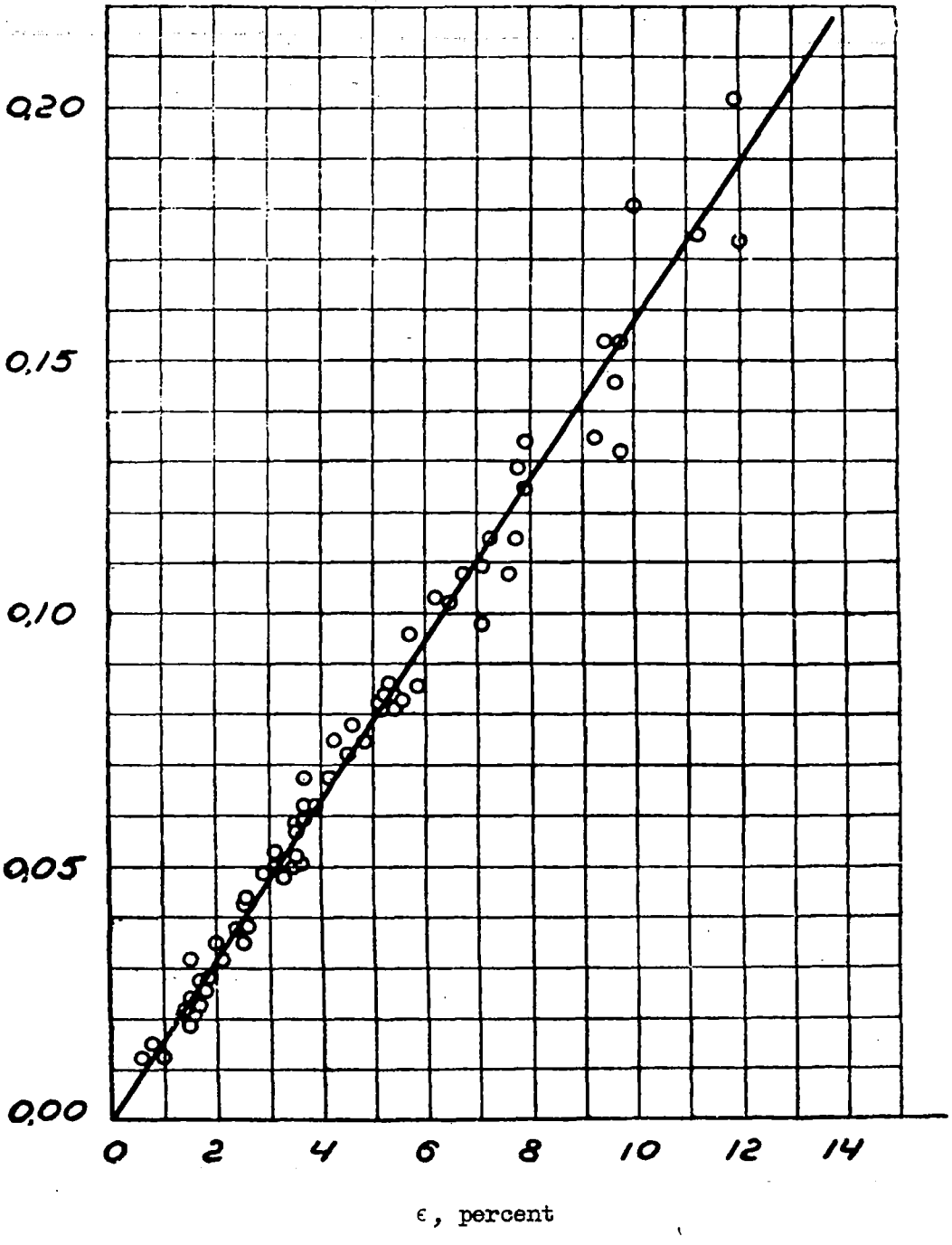

Figure 18. - Dependence of the moment coefficient C_m on ϵ.

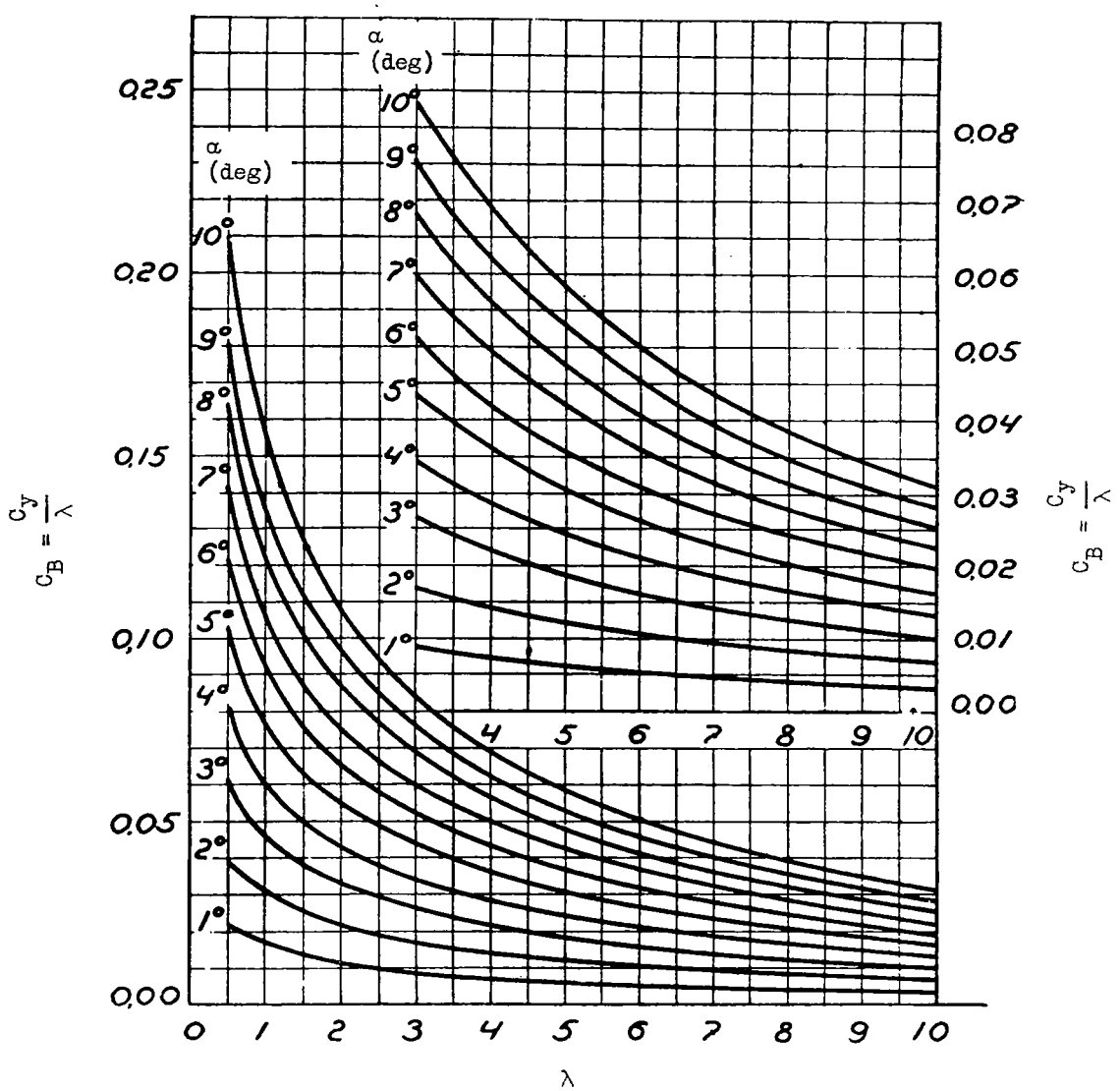

Figure 19. - Dependence of load coefficient $C_B = C_y/\lambda$ on angle of attack α and aspect ratio λ.

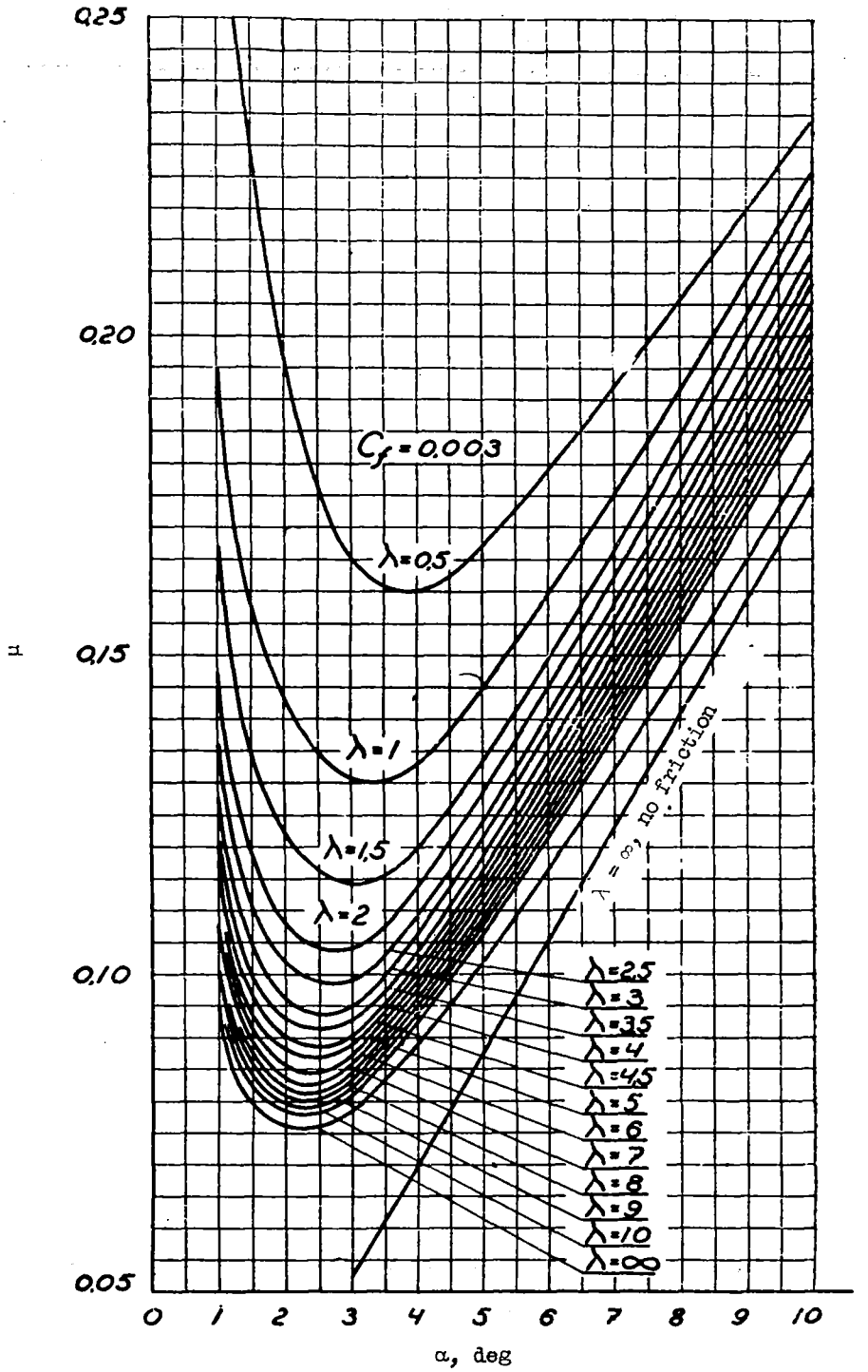

Figure 20. - Dependence of magnitude μ , the reciprocal of the planing efficiency, on angle of attack α and aspect ratio λ. The friction coefficient C_f was assumed constant and equal to 0.003.

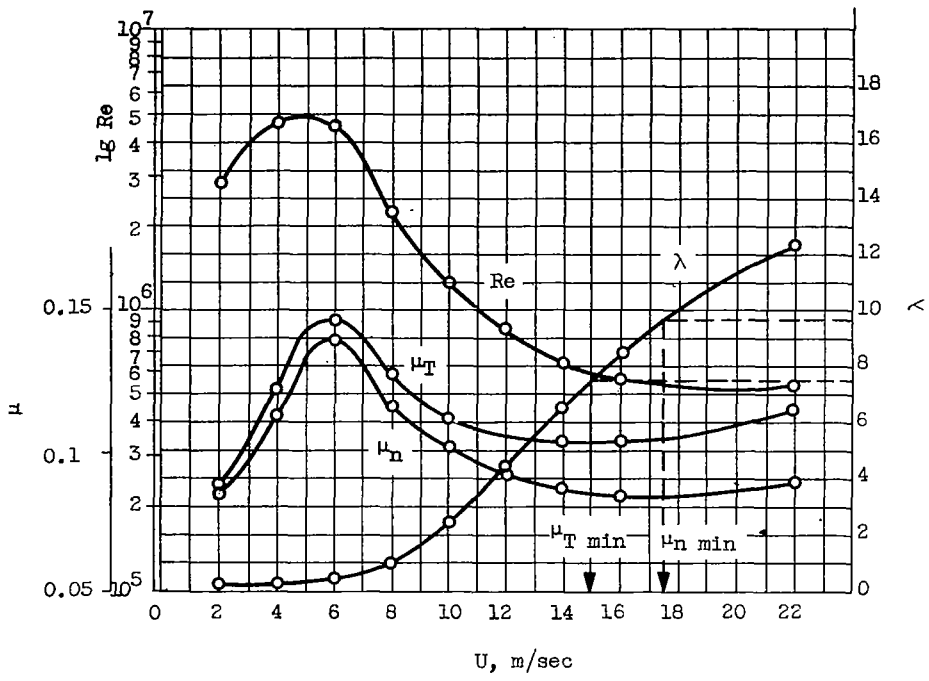

Figure 21. - Curves of Reynolds number R , aspect ratio λ and reciprocal of the planing efficiency μ for a plate of width l = 0.3 meter and load Y = 18 kilograms planing at angle of attack α = 4°.

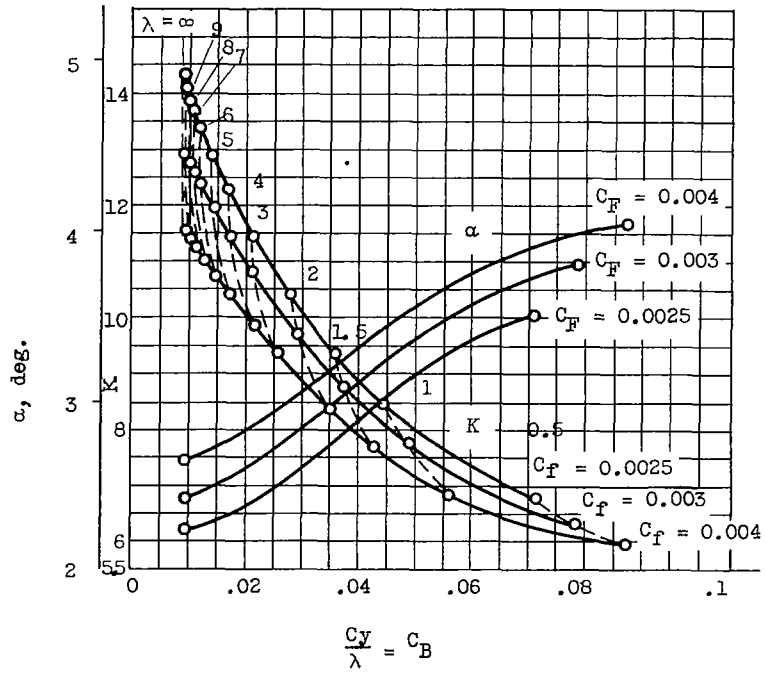

Figure 22. - Variation of optimum angle of attack α and corresponding planing efficiency with friction coefficient C_f and load coefficient C_B.

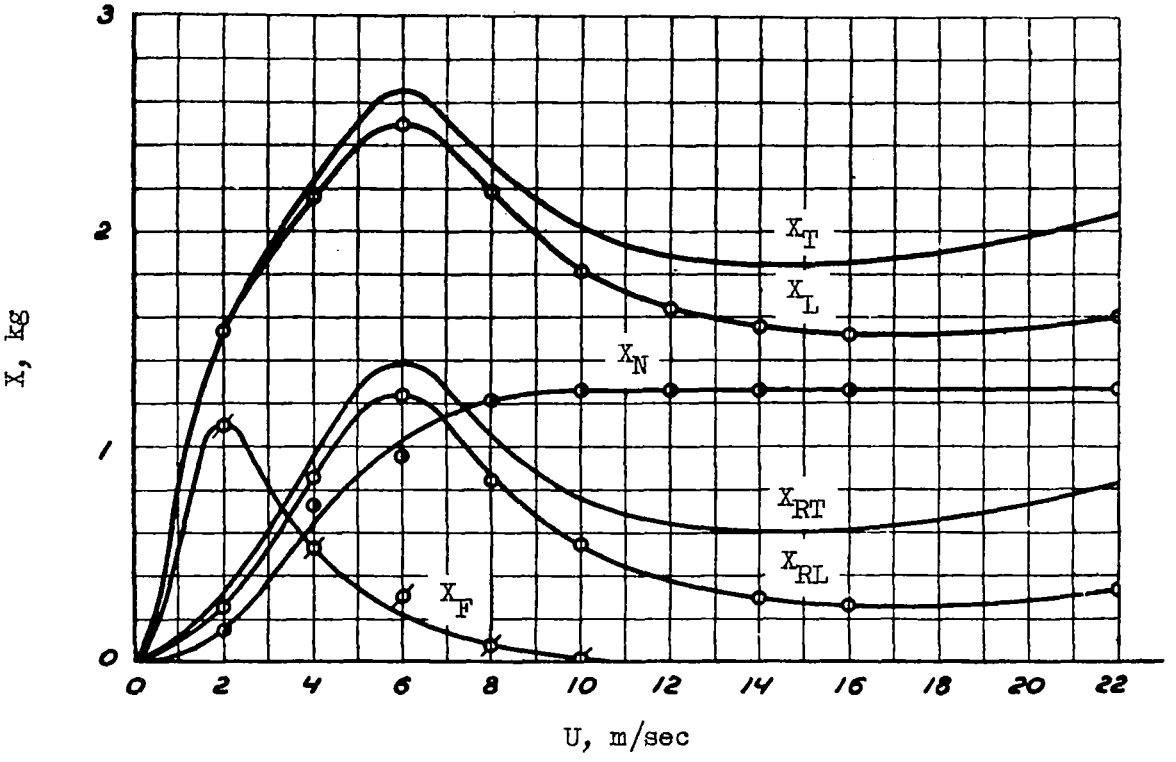

Figure 23. - Computed resistance curves for a plate planing at angle $\alpha = 4^\circ$, load Y = 18 kilograms, and width l = 0.3 meter.

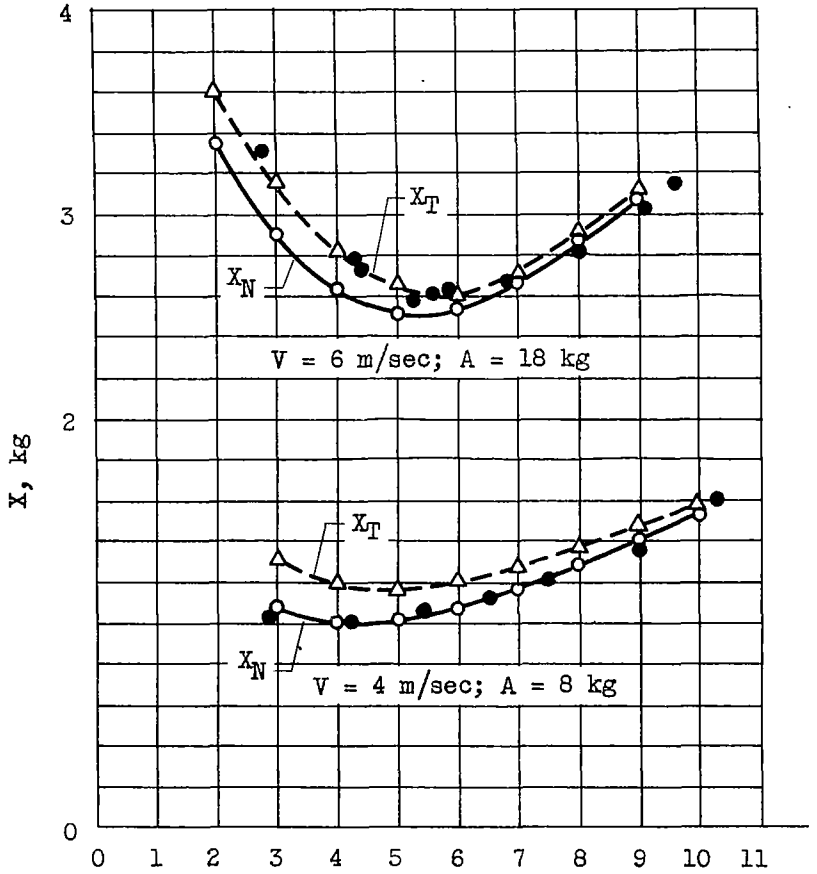

Figure 24.

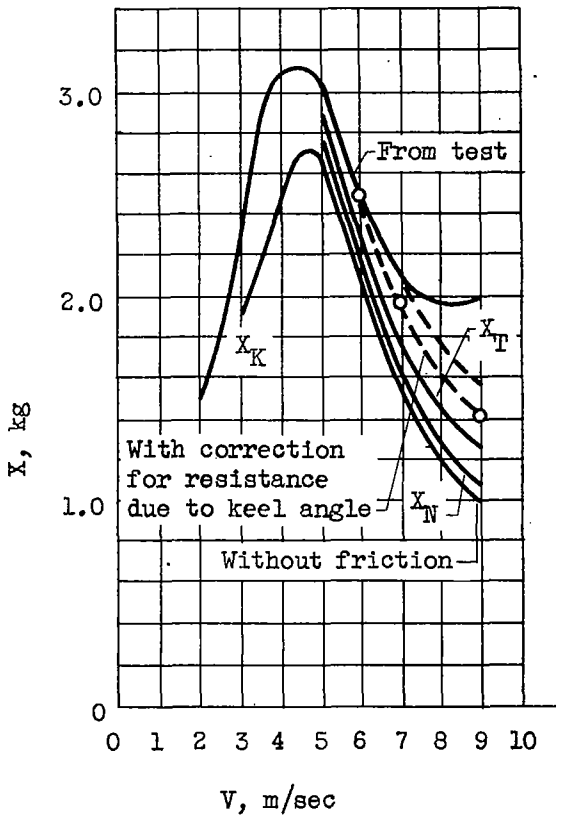

Figure 25.

NACA-Langley - 10-24-50 - 1000